NASA Technical Memorandum 83287

Experimental Determination of Flow-Interference Effects of Wing-Mounted, Two-Dimensional, Full-Capture Propulsion Nacelles in Close Proximity to a Vehicle Body at a Mach Number of 6

Walter A. Vahl

MAY 1982

NASA

NASA Technical Memorandum 83287

Experimental Determination of Flow-Interference Effects of Wing-Mounted, Two-Dimensional, Full-Capture Propulsion Nacelles in Close Proximity to a Vehicle Body at a Mach Number of 6

Walter A. Vahl
Langley Research Center
Hampton, Virginia

National Aeronautics
and Space Administration

**Scientific and Technical
Information Office**

1982

SUMMARY

Experimental tests have been conducted to determine possible aerodynamic interference effects due to the lateral positioning of two-dimensional propulsion nacelles mounted on a wing surface in close proximity to a vehicle body. The tests were conducted at a Mach number of 6 and a Reynolds number of 7×10^6 per foot. The angle-of-attack range for force tests was -9° to 9°. The model configurations consisted of combinations of rectangular and trapezoidal cross-section bodies with a wing swept 65° and a rectangular planform wing. A pair of two-dimensional, flow-through propulsion nacelles simulated full-capture inlet operation. In general, there were only relatively small effects of nacelle placement on the aerodynamic performance of the various configurations. The values of lift-drag ratio L/D ranged from approximately -4 to 4, and the maximum deviation in L/D over the angle-of-attack range for all the configurations was approximately 0.4. The highest deviations in L/D occurred at the more negative angles of attack. At the higher positive angles of attack, representing maximum L/D cruising conditions for nacelle configurations mounted on the upper wing surface, the effect of the lateral positioning of the nacelles was minimal.

INTRODUCTION

As aircraft speeds and altitudes increase, the inlet for the propulsion system becomes an increasingly dominant portion of the overall vehicle configuration. In particular, for vehicles having wing-mounted propulsion nacelles with the inlets located at free-stream or near-free-stream conditions, the required mass flow may result in the inlet frontal area approaching or becoming larger than the projected frontal area of the fuselage. The proper integration of the propulsion system with the vehicle configuration under these circumstances becomes a major design consideration. (See ref. 1.) One concern for wing-mounted propulsion nacelles is the potential for propulsion-nacelle—vehicle-body interference effects due to the proximity of the nacelles to the fuselage.

To obtain a preliminary assessment of possible adverse effects due to wing-surface nacelle positioning, simplified models were constructed and tested at conditions representative of a Mach 6 cruise configuration operating with full-capture inlets. The purpose of the tests was to obtain, in a very simple and expeditious manner, first-order estimates of any possible incremental effects on the overall aerodynamics of a high-speed cruise vehicle resulting from variations in the lateral placement of two-dimensional propulsion nacelles relative to the vehicle body.

SYMBOLS

The longitudinal aerodynamic force data are presented about the stability-axis system. Measurements and calculations were made in the U.S. Customary Units.

C_D drag coefficient, $(\text{Drag})/q_\infty S_r$

C_L lift coefficient, $(\text{Lift})/q_\infty S_r$

L/D	lift-drag ratio, C_L/C_D
M	Mach number
p_1	surface static pressure at flow-survey measurement station
$p_{t,2}$	total pressure behind a normal shock at flow-survey measurement station
$p_{t,\infty}$	free-stream total pressure
q_∞	free-stream dynamic pressure
S_r	reference area (wing planform area, including the fuselage intercept)
V_∞	free-stream velocity
α	angle of attack, deg

WIND-TUNNEL TESTS

Models and Instrumentation

The models were designed as a series of interchangeable components as shown in the photograph of figure 1. Two wing planforms, each having flat upper surfaces, were considered: a rectangular wing providing an unswept leading edge and a wing having a leading-edge sweep of 65°. Two bodies of equal frontal area, which could be mounted on the upper surface of either of the wings, consisted of a rectangular cross-section body having a height-to-width ratio of 1.5 and a trapezoidal cross-section body with a height-to-width ratio of 0.97. The body shapes were selected to provide two different flow channels between the body and nacelles. Only one nacelle shape was considered which represented an upper wing surface, two-dimensional inlet installation on a Mach 6 class cruise configuration operating at design conditions with full inlet capture.

A sketch of the rectangular-wing and rectangular-body combination is shown in figure 2(a). The rectangular wing with the trapezoidal body is shown in figure 2(b). For both rectangular-wing configurations, the nacelles were positioned longitudinally so that the most forward edge of the inlet was on the wing leading edge. The model configurations using the swept wing with the rectangular and trapezoidal bodies are sketched in figures 2(c) and 2(d), respectively. For the swept wing, with each body, the nacelles were positioned longitudinally so as to represent both an inlet installation behind the wing leading edge as well as an inlet installed ahead of the wing leading edge. An example of the nacelle inlets mounted aft of the wing leading edge is shown in figure 2(c). The inlet mounted forward of the wing leading edge is shown in figure 2(d). Provisions were made so that the nacelles could be installed on the wings at several lateral positions relative to the bodies. The sketches in figure 2 show the nacelles mounted in only one of the possible lateral positions. The complete range of lateral placement of the nacelles with respect to the rectangular and trapezoidal bodies is shown in figures 3(a) and 3(b), respectively. For the rectangular body, the nacelle near-wall lateral position varied from being flush with the body wall to a maximum distance of 0.90 in. from the body and, for the trapezoidal body, from being flush with the body base to a maximum lateral displacement of 0.60 in.

Details of the nacelle geometry are shown in figure 4. All fore and aft edges of the nacelle were sharp. The projected frontal areas of the nacelle surfaces, normal to the free-stream direction, with the exception of the upper cowl surface, were exposed to the nacelle internal-flow stream only.

The model instrumentation consisted of a six-component strain-gage balance mounted internally within the fuselage for determining the forces and moments acting on the model. Four base-pressure probes, installed within approximately 0.06 in. of the base surface and distributed over approximately equal areas, were in place during all balance measurements. The base pressures were averaged and applied to the axial-force determination to correct it to the equivalent of free-stream static pressure acting over the base area.

A flow-survey rake, consisting of six pitot tubes, could be mounted on one upper side of each of the wings in place of the nacelle. The tubes were spaced so as to obtain data over the approximate lateral range of the nacelle positions at the inlet midheight. A series of six static orifices were provided in the wing upper surfaces so as to be in the same vertical plane and at the same longitudinal station as each of the total-pressure probes. Details of the flow-measurement locations are shown in figure 5. All measurements were taken 1.0 in. aft of the wing leading edge.

Test Conditions and Procedures

The tests were conducted in the Langley 20-Inch Mach 6 Tunnel which is a blow-down type and has a two-dimensional nozzle. The test section is 20 in. square. Additional details of the tunnel can be found in reference 2.

Nominal values of the stagnation pressure and temperature were 425 psi and 425°F, respectively. These conditions correspond to a free-stream Reynolds number of 7×10^6 per ft. Data were taken through an angle-of-attack range from -12° to 12° at a sideslip angle of 0°.

Forces and moments were measured with an internally mounted six-component strain-gage balance. The models were remotely actuated and the angle of attack was determined by using prisms mounted on the models which reflected light on to a calibrated chart. A pitot-pressure probe, located in the test section so as to avoid interference with the models, was used to determine the Mach number for each test point. No corrections were made to the data for the internal flow through the nacelle ducts.

The tests were conducted in two phases. The first phase consisted of oil-flow studies, with the nacelles installed, as a means of obtaining an insight to potential flow-interference regions. The nacelles were then removed and flow pressure surveys were obtained over the proposed nacelle positions for each wing-body configuration in an effort to determine the uniformity of local flow conditions at the nacelle-duct entrances. The second test phase consisted of measuring the aerodynamic forces acting on the models for the various nacelle positions by using an internally mounted strain-gage balance. It was reasoned that if the flow properties were approximately uniform over the range of lateral positions of the nacelles, then any effect of momentum-force changes in the internal flow in the duct would be minimal. Comparisons could then be made to determine the approximate force increments due to flow-interference effects which might occur as the nacelles are moved in close proximity to the vehicle body.

DISCUSSION OF RESULTS

Oil Flows

To obtain an insight into local-flow disturbances resulting from installing the nacelles at several lateral positions relative to the body sidewalls, oil-flow photographs were obtained over the range of angle of attack for several test configurations. For improved contrast, each model was first painted a dark background color and then spotted uniformly with a mixture of oil and white pigment. The model was then injected into the wind-tunnel test-section flow, positioned at the proper angle of attack, and observed by using a remote television monitor. After the oil mixture had spread across the model surfaces and assumed the direction of the local surface flow, the model was immediately retracted from the test section with no change in model attitude. Photographs were then taken of the resulting oil-flow patterns. To reduce the wind-tunnel test time required, each model configuration had its two nacelles mounted at different lateral positions; i.e., one nacelle was at its farthest position from the body, while the opposite nacelle was at an intermediate position relative to the body.

Representative oil-flow photographs of two of the model configurations are shown in figure 6. Figure 6(a) shows the rectangular wing and trapezoidal body at $\alpha = 6°$ taken at two different camera-viewing angles so that both sides of the body and nacelle sidewalls can be seen for each of the nacelle positions. The nacelle at the top of the photograph is positioned flush with the body base, whereas the nacelle at the bottom of the photograph is located at its farthest position from the body sidewall. Similar photographs of the swept wing with the trapezoidal body at $\alpha = 0°$ are shown in figure 6(b).

It is apparent that there are distinctive differences in the appearance of the oil-flow patterns in the region between the nacelle and body sidewalls for both model arrangements at each of the angles of attack. For the rectangular wing configuration at $\alpha = 6°$ (fig. 6(a)), it appears that vortex flow from the forward lower section of the body washes both the body and nacelle sidewalls for the nacelle at the top of the photograph which is flush with the body base. For the nacelle at the bottom of the photograph, which is farthest from the body, the vortex flow seems to have little effect on the nacelle inner sidewall.

For the swept-wing configuration at $\alpha = 0°$ (fig. 6(b)), there seems to be no indication of vortex flow on the fuselage and, in the case of the nacelle at the bottom of the photograph which is farthest from the body, the passage between the nacelle and body seems to offer little disturbance to the flow as evidenced by the smooth oil-flow traces. In contrast, for the nacelle at the top of the photograph which is flush with the body base, the external flow seems to be forced upward with the smaller passage between the nacelle and body perhaps offering greater interference to the flow as evidenced by the lack of spreading of the oil-pigment spots. Similar-type oil-flow patterns were observed with the rectangular body for each of the two wing shapes.

At each of the angles of attack illustrated in figure 6, the differences in the local flow patterns for the nacelles located in close proximity to the body and for the nacelles located farther from the body would suggest that there may be an effect on the overall aerodynamic forces acting on the configurations because of the lateral positioning of the propulsion nacelles. To determine the magnitude of possible interference effects on the overall configuration aerodynamics by using an internally

mounted balance, the assumption was made that the flow entering the nacelle ducts would be sufficiently uniform so as to minimize the effect of internal-momentum changes over the range of nacelle lateral placement. To verify this assumption, flow-survey pressure measurements were made with the nacelles removed prior to the force measurements.

Pressure Distributions

The pressure distributions obtained during the flow-survey phase of the test are shown in figure 7. The total-pressure measurements were made at a height of 0.75 in. from the wing surface which was the midpoint of the inlet height. The static-pressure measurements were made on the wing upper surface in the same vertical plane as the total-pressure probes and at the same longitudinal station. The data are plotted against the lateral distance of the measurement station from the body center-line reference. Calculations to estimate the body boundary-layer thickness at the probe station were made by assuming incompressible flow on a flat plate. The boundary-layer thickness calculated was approximately 0.23 in. at 0° angle of attack.

The variation in the total- and static-pressure profiles appears to be rather consistent for each of the four wing-body combinations. The static-pressure levels are fairly constant with lateral position from the body wall for each of the positive angles of attack for all configurations. At a negative angle of attack of -6°, the pressures are fairly constant except for the two measurement positions nearest the body. More-pronounced deviations in static-pressure levels occur at $\alpha = -12°$.

The total-pressure values are fairly uniform over the lateral-measurement positions outside the estimated boundary layer for angles of attack ranging from approximately -6° to 6°. Considerable fluctuation in the total-pressure values with lateral position occurs at angles of attack of -12° and 12°. Based on the trends of the static- and total-pressure survey values, it was decided that the force tests should be restricted to an angle-of-attack range from -9° to 9°. The assumption was thus made that the variation in pressure levels occurring over the lateral range of nacelle positions would have a minimal effect on the variation of the nacelle entrance and exit internal-momentum forces as compared with the forces occurring because of nacelle-body flow interference.

Aerodynamic Effects

The aerodynamic coefficients obtained with the internally mounted strain-gage balance are presented in figures 8 and 9. Figure 8 gives typical force data for two of the configurations illustrated in figure 2. The data are plotted as a function of the lateral position of the nacelle for angles of attack of -9°, 0°, and 9°. In figure 9, data for all configurations are presented at all test angles of attack for the most outboard and most inboard nacelle position only. In reviewing these data, it becomes apparent that there are only relatively small effects of nacelle placement on the aerodynamic performance of the total configuration. When referring to figure 8(a), which is typical of the rectangular-wing configurations, it can be seen that there is no change in the value of L/D at $\alpha = 0°$ for the trapezoidal body over the range of nacelle positions. At an angle of attack of 9°, this configuration shows a maximum deviation in L/D values of only approximately 0.1 over the complete range of nacelle positions. Similar results were obtained with the rectangular body mounted on the rectangular wing.

The swept-wing configurations exhibited a slightly higher deviation in L/D values at $\alpha = 0°$ for the range of nacelle positions. Typical data for the rectangular body on the swept wing (fig. 8(b)) show a maximum variation at $\alpha = 0°$ of approximately 0.3. At $\alpha = 9°$, the variation in L/D for this configuration over the range of nacelle positions is approximately 0.1. Similarly, for the trapezoidal body mounted on the swept wing, the maximum deviations in L/D were 0.4 at $\alpha = 0°$ and 0.2 at $\alpha = 9°$.

The aerodynamic performance parameters over the angle-of-attack range for the two extreme positions of nacelle lateral placement, i.e., the closest inboard position to the body sidewalls and the farthest outboard position from the body sidewalls (fig. 9), show that the small effects on the total-configuration aerodynamics due to nacelle position progress uniformly throughout the angle-of-attack range. The L/D values, which reflect the combined effect of nacelle-interference effects on both the lift and drag forces, show that the effects are mainly present at the negative angles of attack. For the higher positive angles of attack, representing maximum L/D cruising conditions for configurations with nacelles mounted on the upper wing surface, the effect of the lateral positioning of the nacelles is minimal.

In reference 3, wind-tunnel tests performed on aerodynamic configured missiles over a Mach number range from 0.55 to 5.5 found that the use of right-angle unfaired corners on streamwise surfaces such as wing-inlet junctions had no significant effect on measured drag values. These findings are further supported with the present tests at $M = 6$ where the various-sized right-angle flow channels occurring between the body and propulsion-nacelle wall showed no significant drag differences.

Although the results presented shown only small aerodynamic effects due to nacelle-body interference, this in itself is significant. From analysis of the oil-flow patterns and flow-survey pressure distributions, one might suspect that there could be considerable influence of the nacelle placement on the overall vehicle aerodynamics. The reader should be cautioned at this point, however, that these tests represented the condition of full-capture inlets operating at design conditions only, and hence, the effect of inlet spillage which occurs when the vehicle operates at below-design Mach number conditions was not addressed. Additionally, since most of the body and nacelle external surfaces were aligned with the stream, the effects of shock interactions were minimized.

SUMMARY OF RESULTS

Experimental tests have been conducted to determine possible aerodynamic interference effects due to the lateral positioning of two-dimensional propulsion nacelles mounted on a wing surface in close proximity to a vehicle body. The tests were conducted at conditions representing Mach 6 cruise with full-capture inlets. The free-stream Reynolds number was 7×10^6 per ft. For force tests, the angle-of-attack range was -9° to 9°. The configurations consisted of a rectangular wing and a wing with the leading edge swept 65°, on each of which could be mounted a rectangular cross-section body or a trapezoidal cross-section body. Based on the data obtained in the tests, the following results are considered significant:

1. Generally, over the range of nacelle lateral placement, as well as over the test angle-of-attack range, there are only relatively small effects on the overall aerodynamic performance of the configurations, occurring mainly at the more negative angles of attack α.

2. Specifically, for the rectangular wing at $\alpha = 0°$, there is no change in the lift-drag L/D value for either the rectangular or trapezoidal body over the range of nacelle lateral positions. At $\alpha = 9°$, the maximum deviation in L/D was approximately 0.1.

3. For the swept wing, the maximum variation in L/D at $\alpha = 0°$ over the lateral range of nacelle placements was 0.4, whereas at $\alpha = 9°$, the maximum variation was 0.2.

4. For the higher positive angles of attack, representing maximum L/D cruising conditions for configurations with nacelles mounted on the upper wing surface, the effect of the lateral positioning of the nacelles is minimal.

5. Although the effects of nacelle lateral placement on the aerodynamic performance of the vehicle are relatively small, it should be borne in mind that the test conditions simulated a full-capture inlet only and that the nacelle-body interference effects of off-design inlet operation with inlet-flow spillage were not addressed. Additionally, since most of the external surfaces of the body and nacelle were aligned with the stream, the effects of shock interactions were minimized.

Langley Research Center
National Aeronautics and Space Administration
Hampton, VA 23665
April 13, 1982

REFERENCES

1. Weidner, John P.: Propulsion/Airframe Integration Considerations for High Altitude Hypersonic Cruise Vehicles. AIAA Paper 80-0111, Jan. 1980.

2. Goldberg, Theodore J.; and Hefner, Jerry N. (appendix by James C. Emery): Starting Phenomena for Hypersonic Inlets With Thick Turbulent Boundary Layers at Mach 6. NASA TN D-6280, 1971.

3. Krieger, R. J.: Summary of Design and Performance Characteristics of Aerodynamic Configured Missiles. AIAA-81-0286, Jan. 1981.

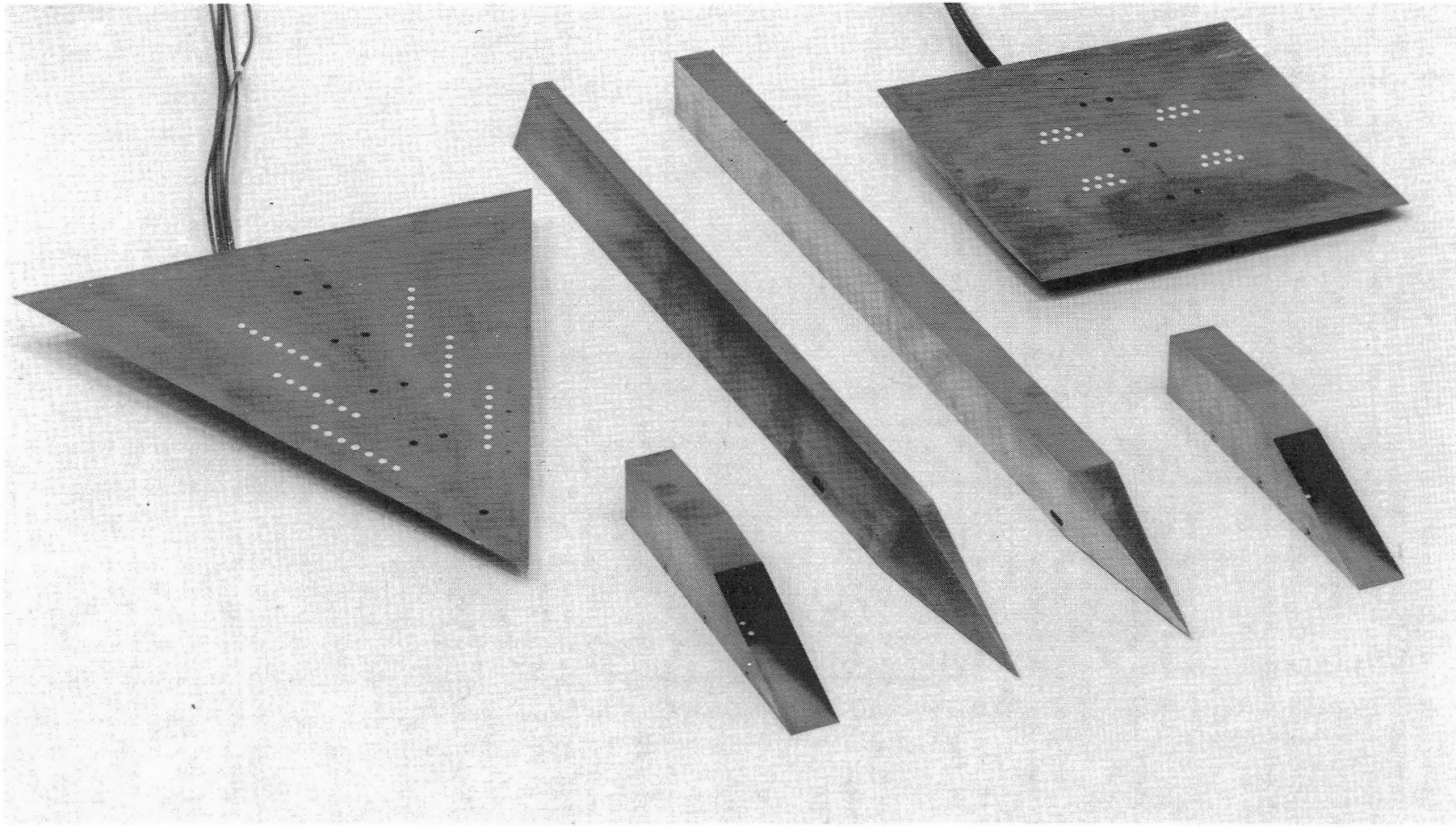

L-79-4548

Figure 1.- Photograph of the model components.

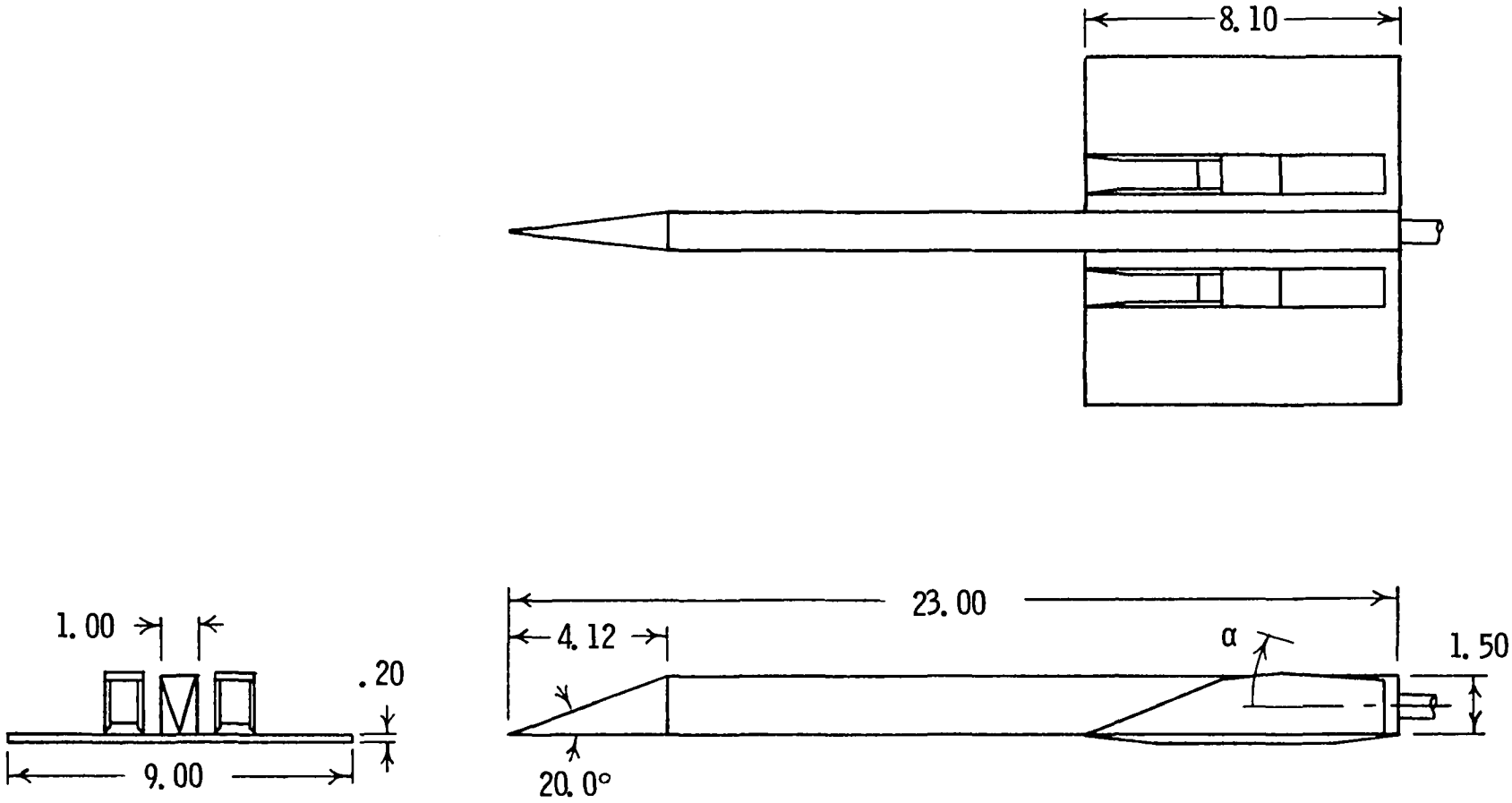

(a) Rectangular body and rectangular wing.

Figure 2.- Sketches of the model configurations. All dimensions are given in inches unless otherwise noted.

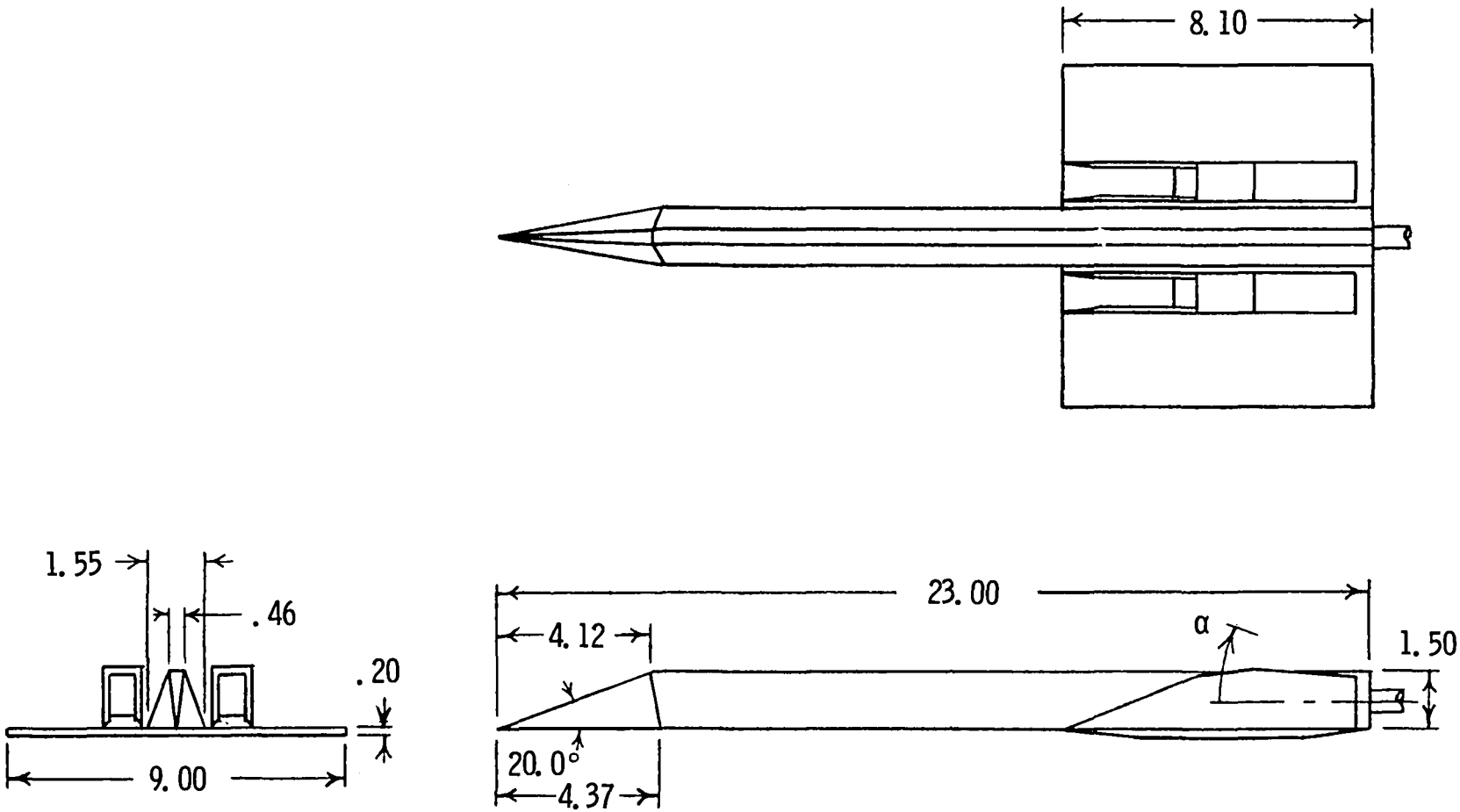

(b) Trapezoidal body and rectangular wing.

Figure 2.- Continued.

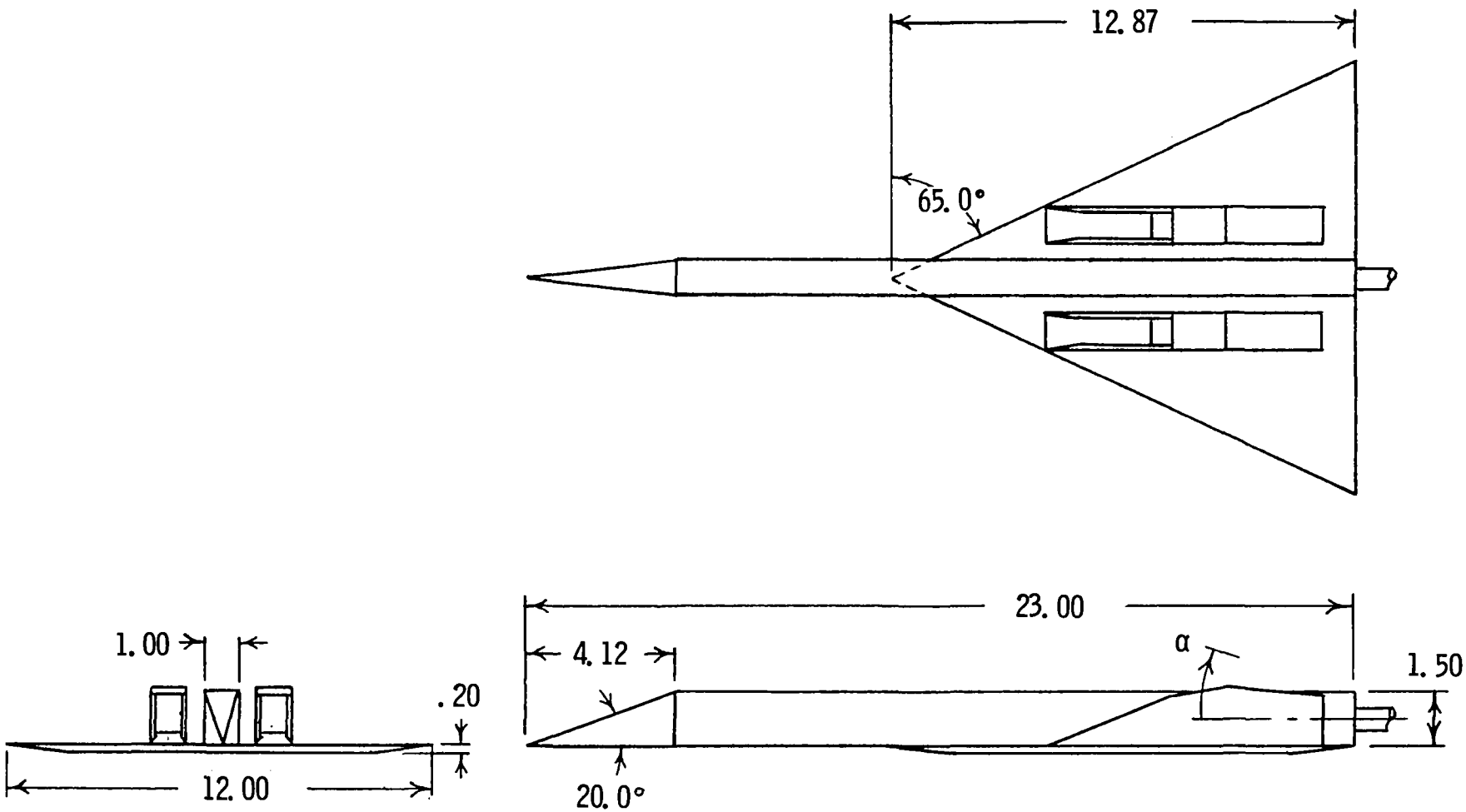

(c) Rectangular body and swept wing; nacelle inlets aft of wing leading edge.

Figure 2.- Continued.

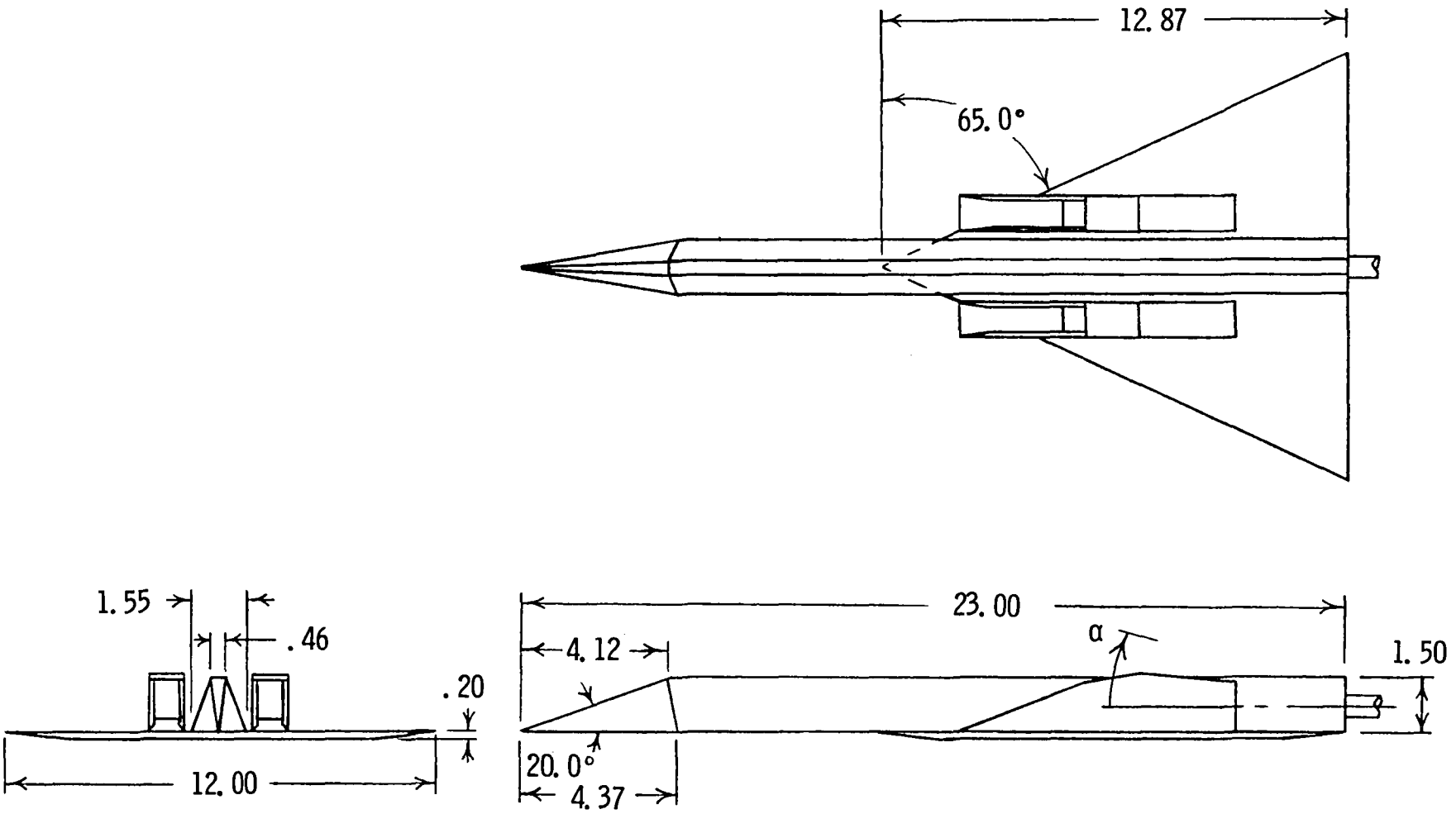

(d) Trapezoidal body and swept wing; nacelle inlets forward of wing leading edge.

Figure 2.- Concluded.

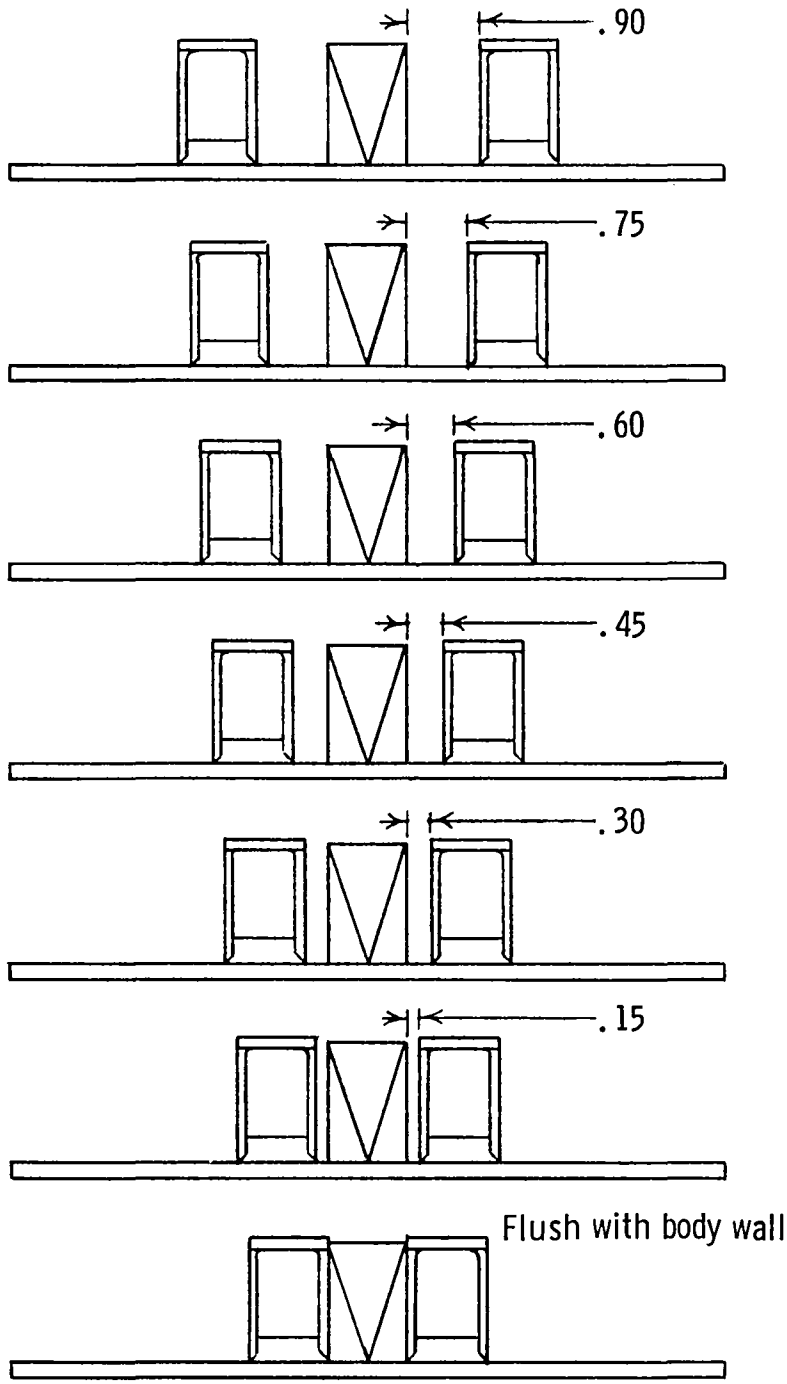

(a) Rectangular body.

Figure 3.- Sketches of the nacelle lateral positions.
All dimensions are given in inches.

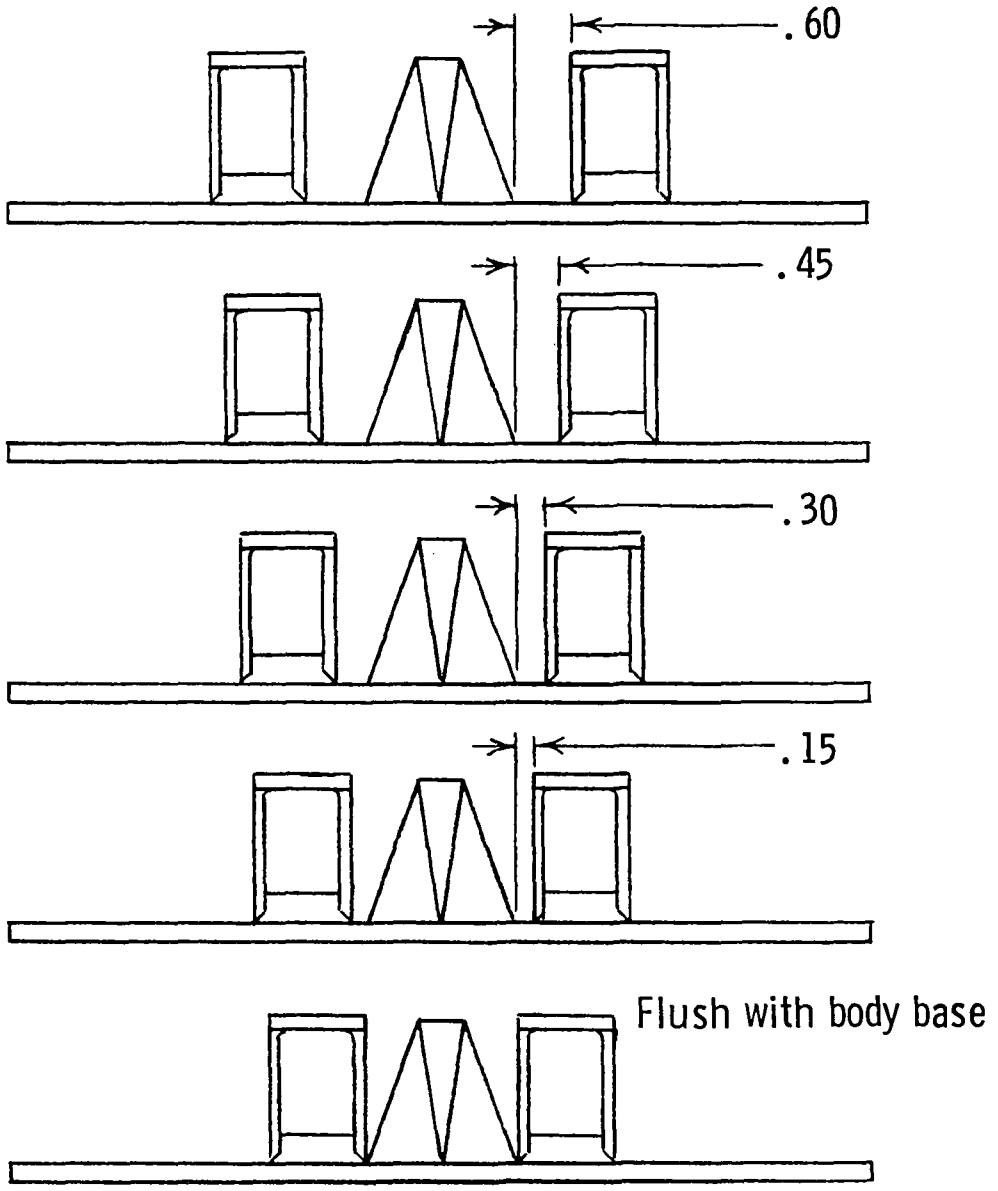

(b) Trapezoidal body.

Figure 3.- Concluded.

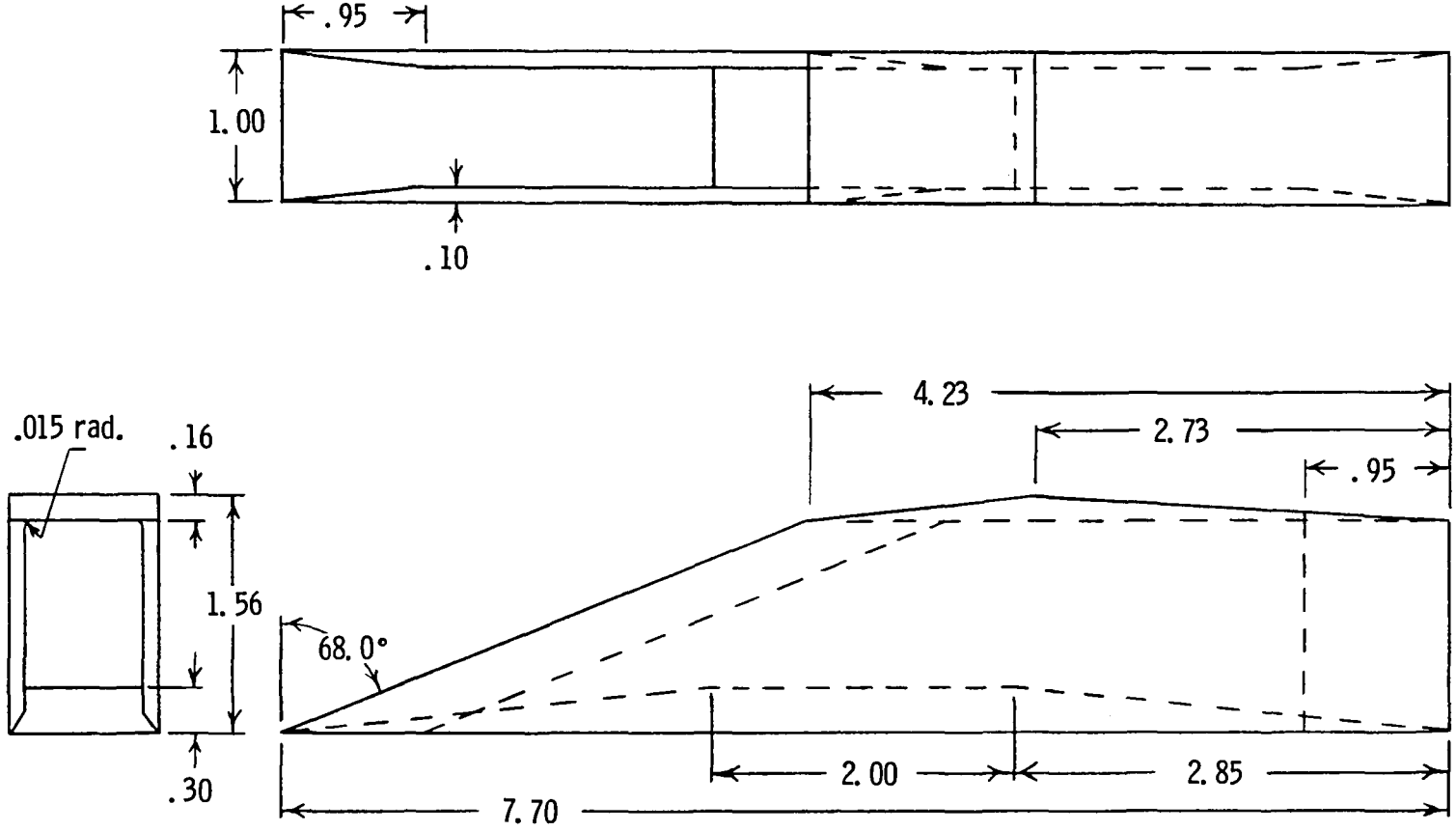

Figure 4.- Details of the nacelle geometry. All dimensions are given in inches unless otherwise noted.

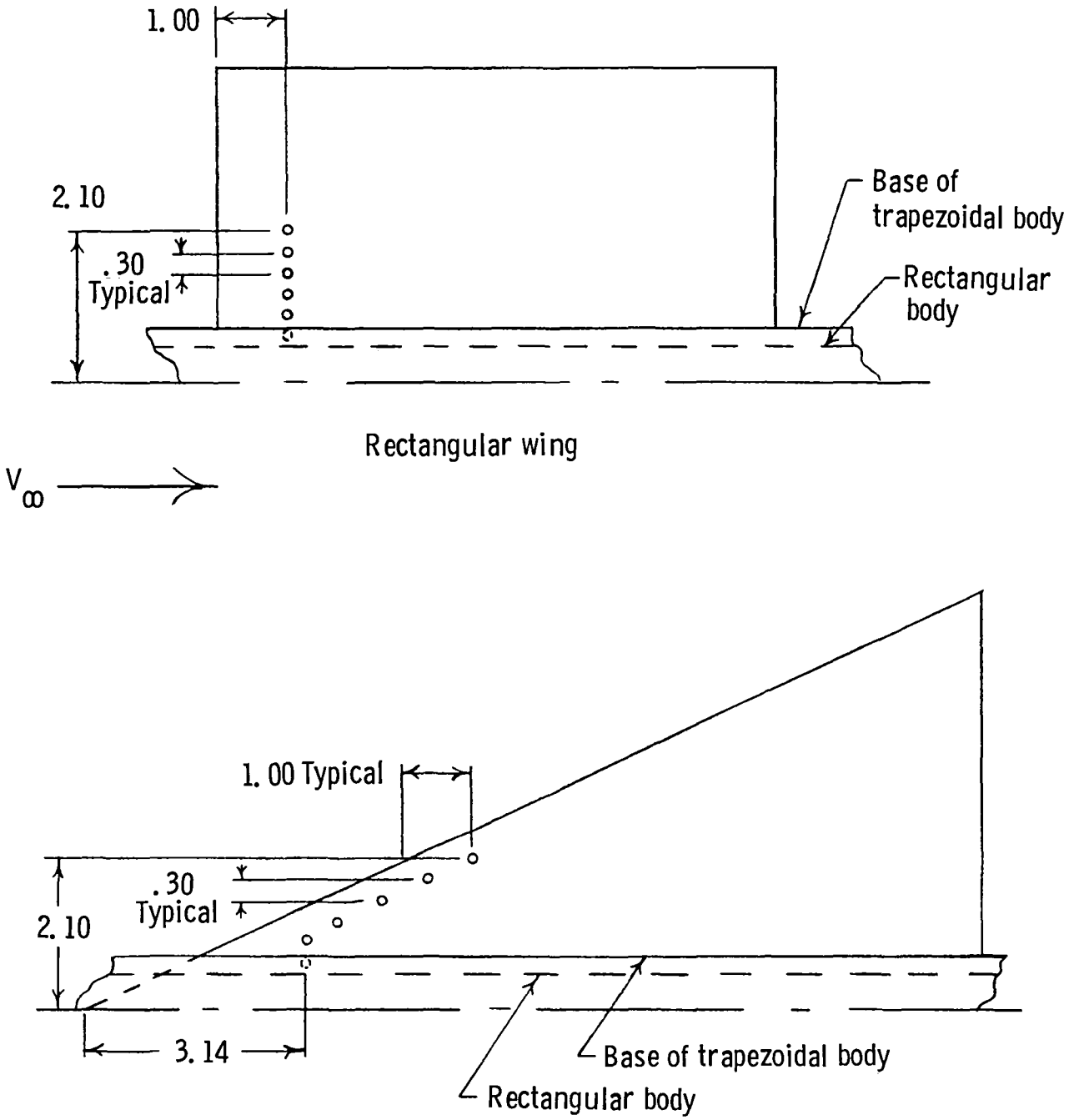

(a) Top view.

Figure 5.- Details of the flow-measurement locations. All dimensions are given in inches.

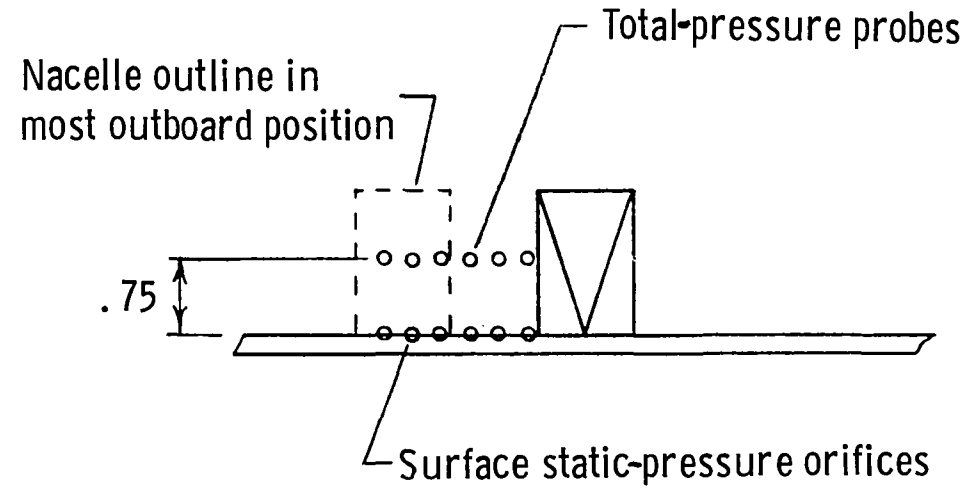

Rectangular body

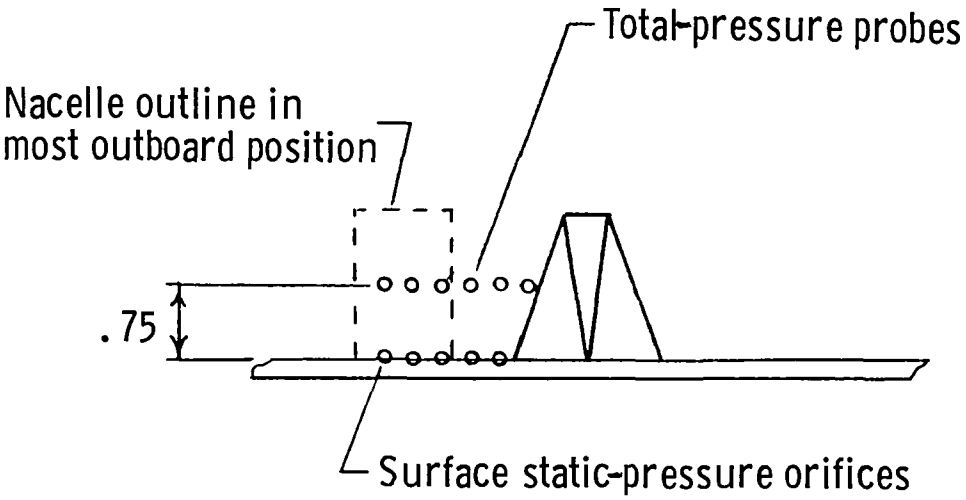

Trapezoidal body

(b) Front view.

Figure 5.- Concluded.

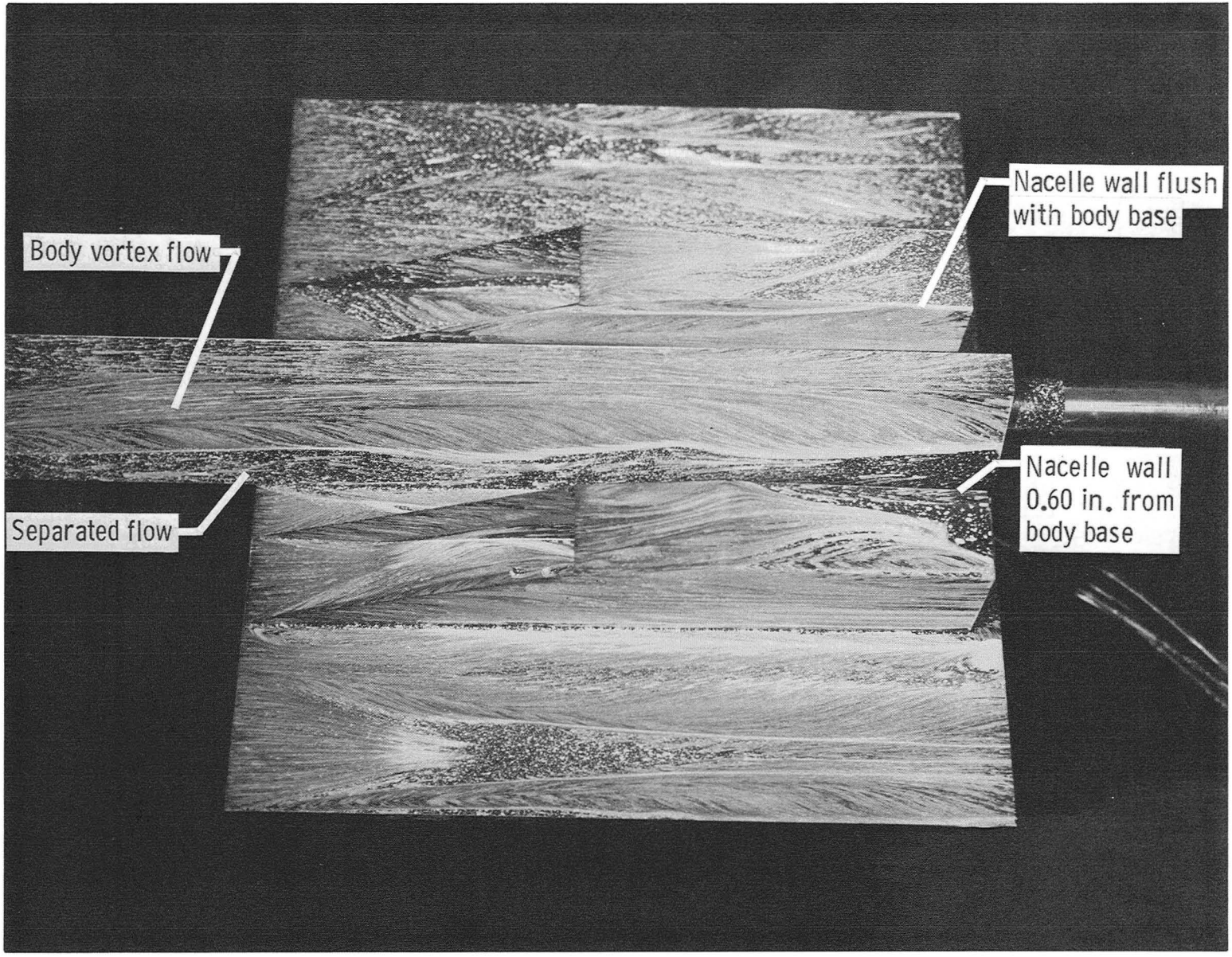

L-82-130

(a) Trapezoidal body and rectangular wing at $\alpha = 6°$.

Figure 6.- Representative oil-flow photographs.

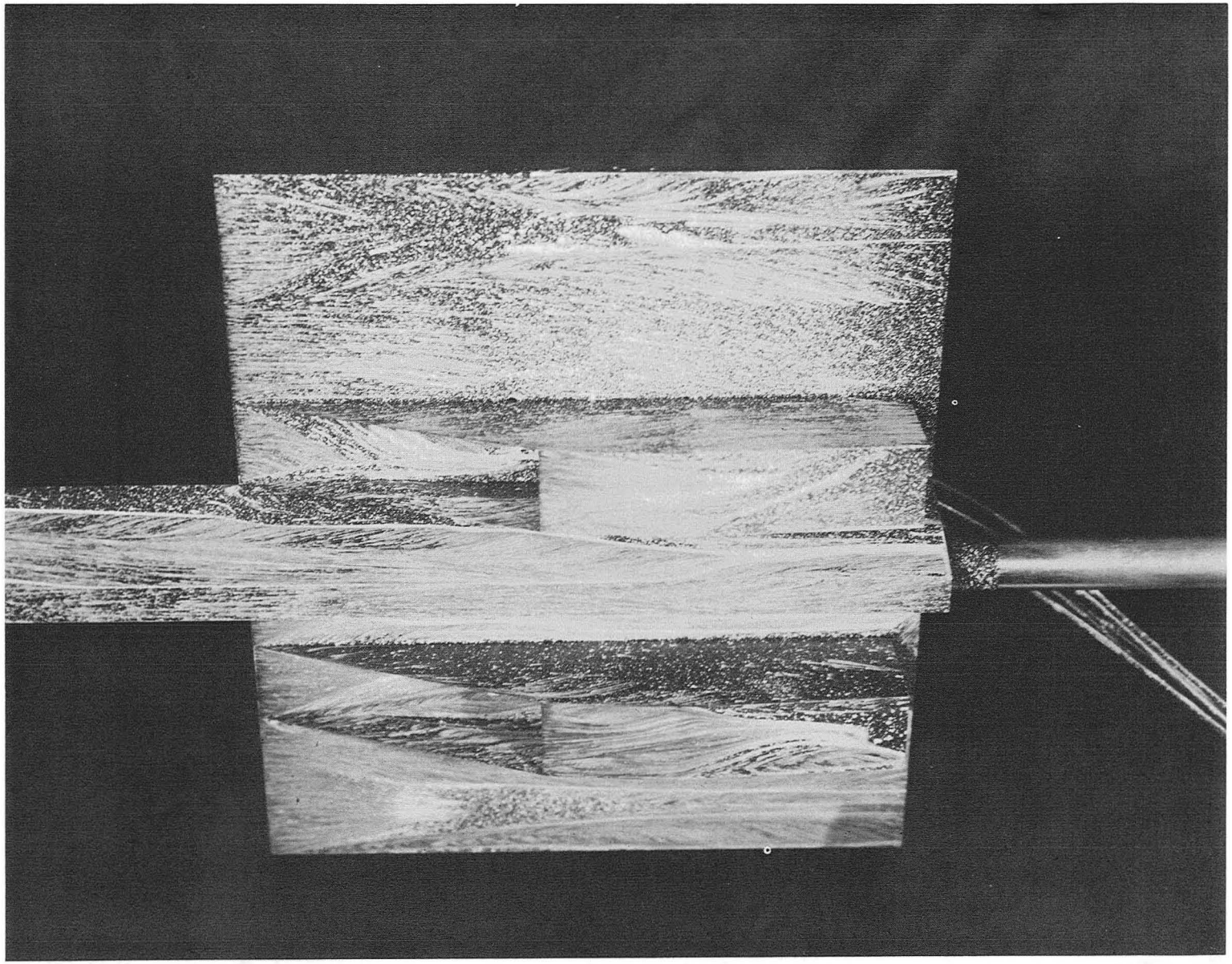

L-82-131

(a) Concluded.

Figure 6.- Continued.

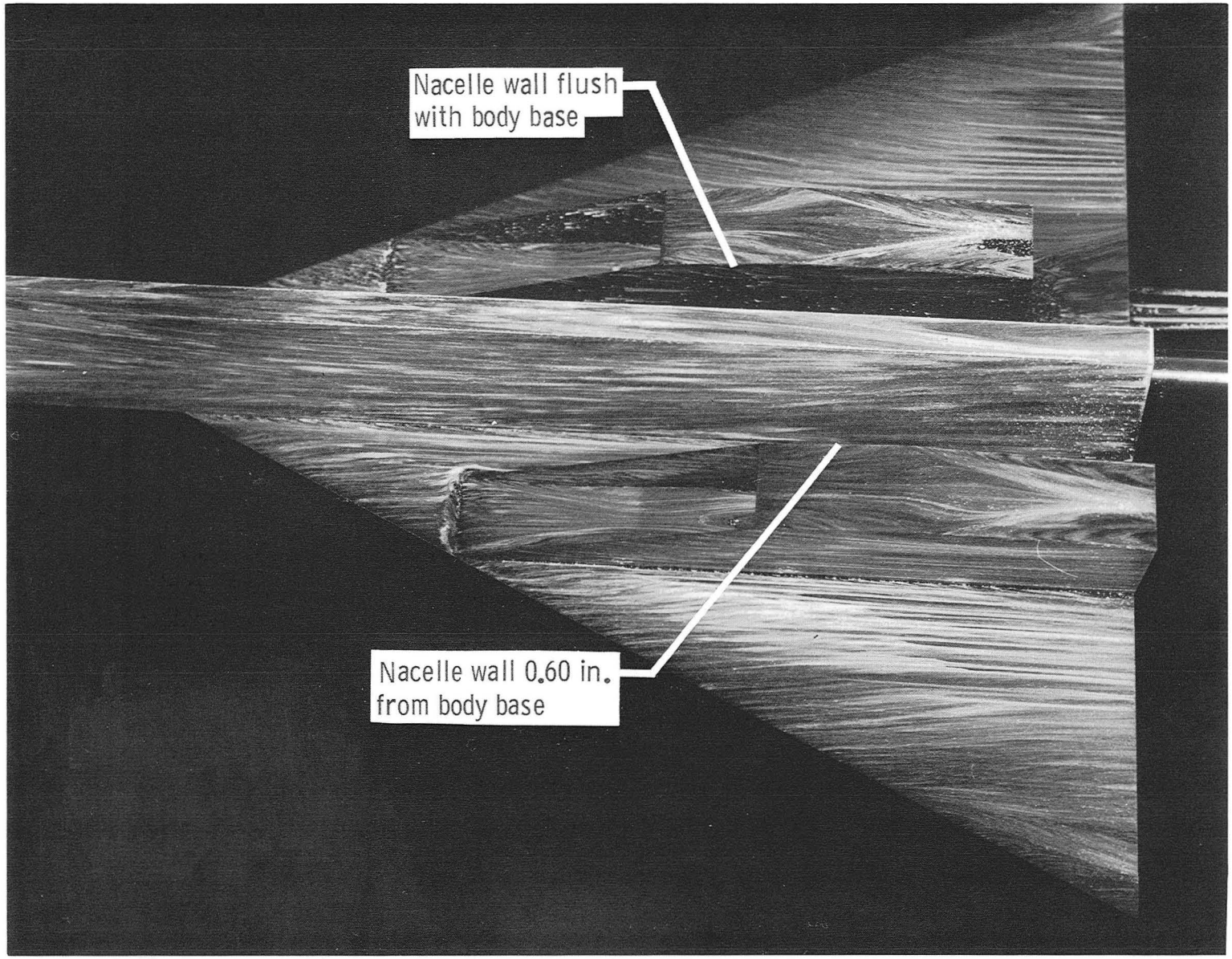

L-82-132

(b) Trapezoidal body and swept wing at $\alpha = 0°$; nacelle inlets aft of wing leading edge.

Figure 6.- Continued.

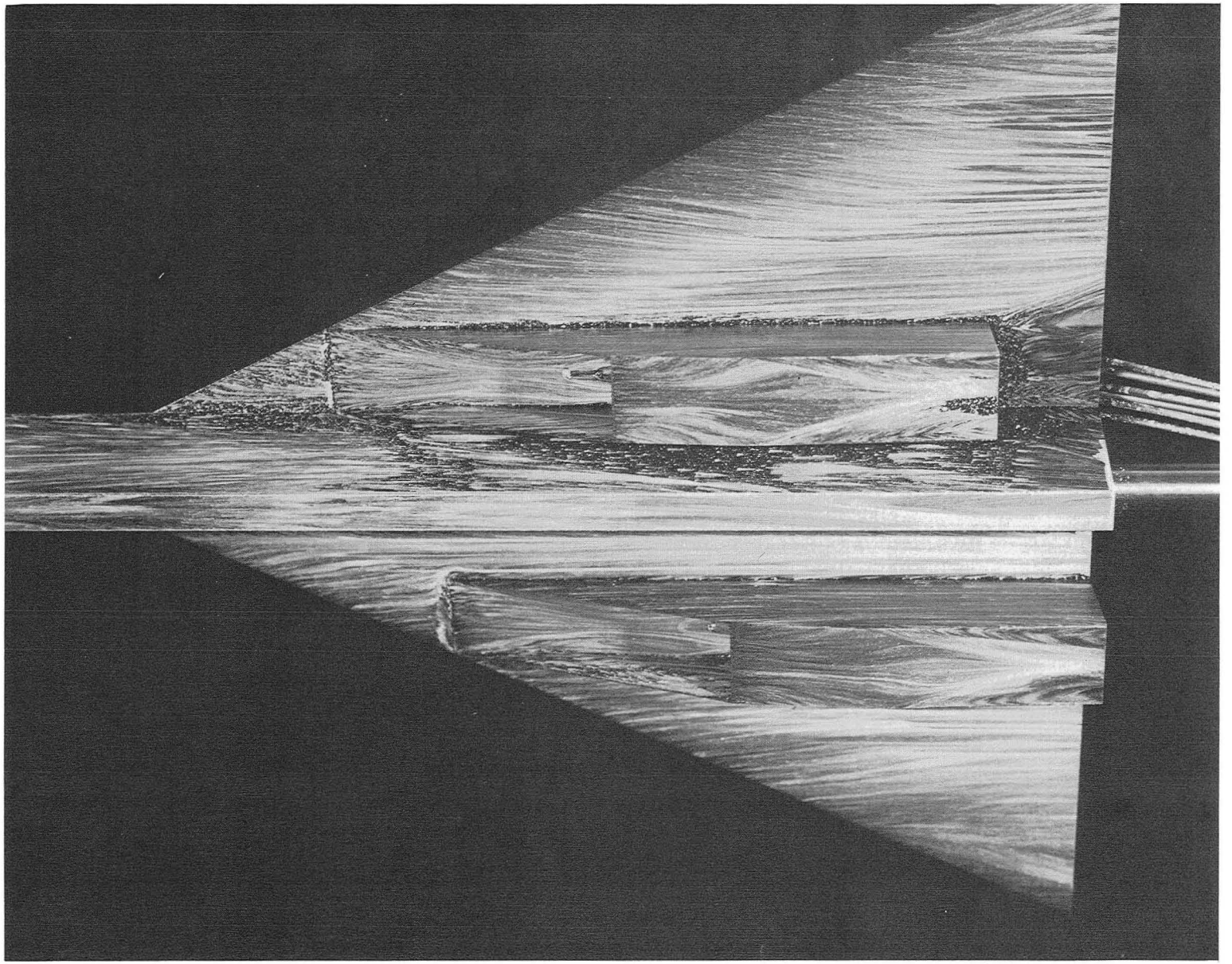

L-82-133

(b) Concluded.

Figure 6.- Concluded.

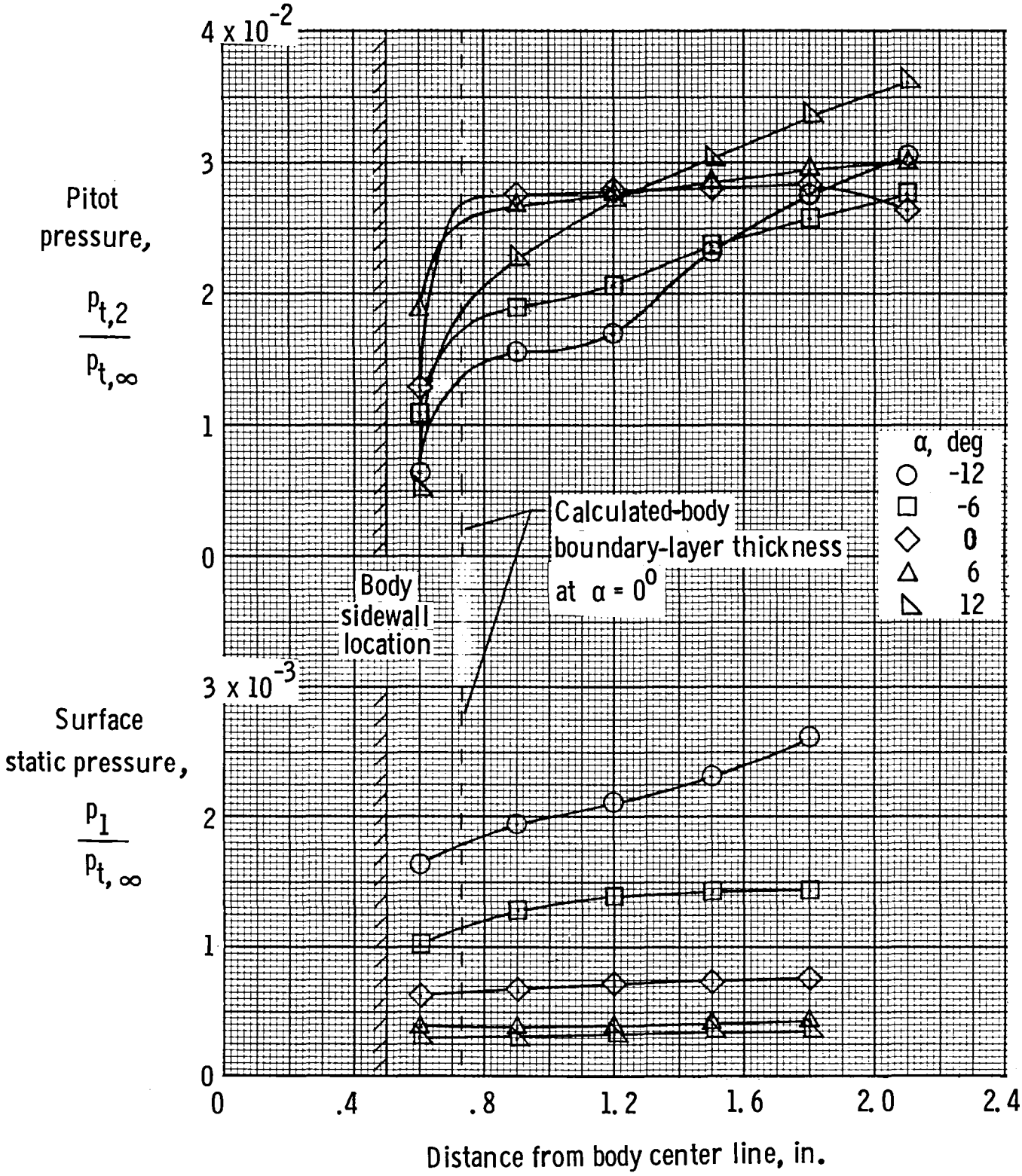

(a) Rectangular body and rectangular wing.

Figure 7.- Pressure distributions at nacelle-inlet positions.

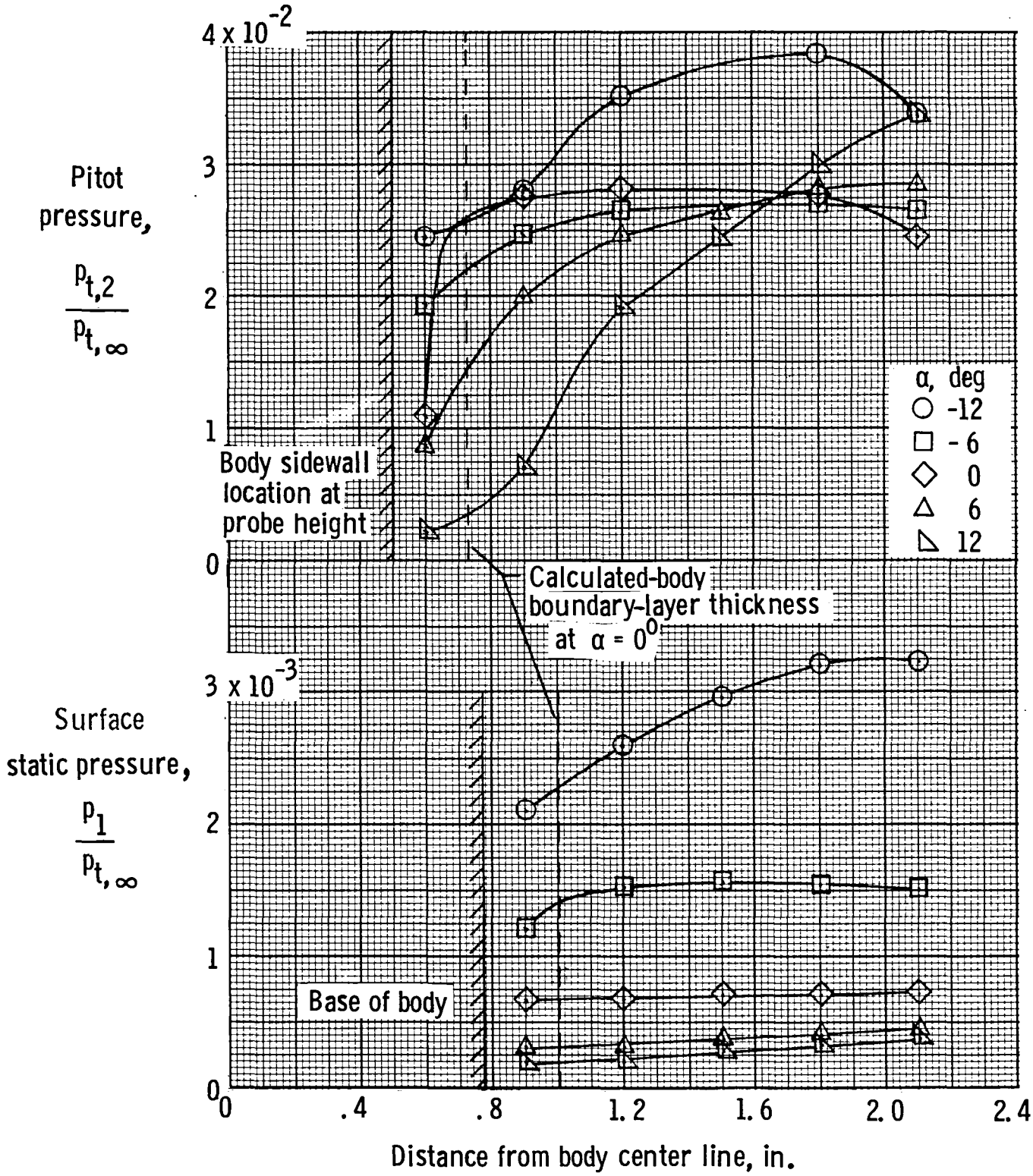

(b) Trapezoidal body and rectangular wing.

Figure 7.- Continued.

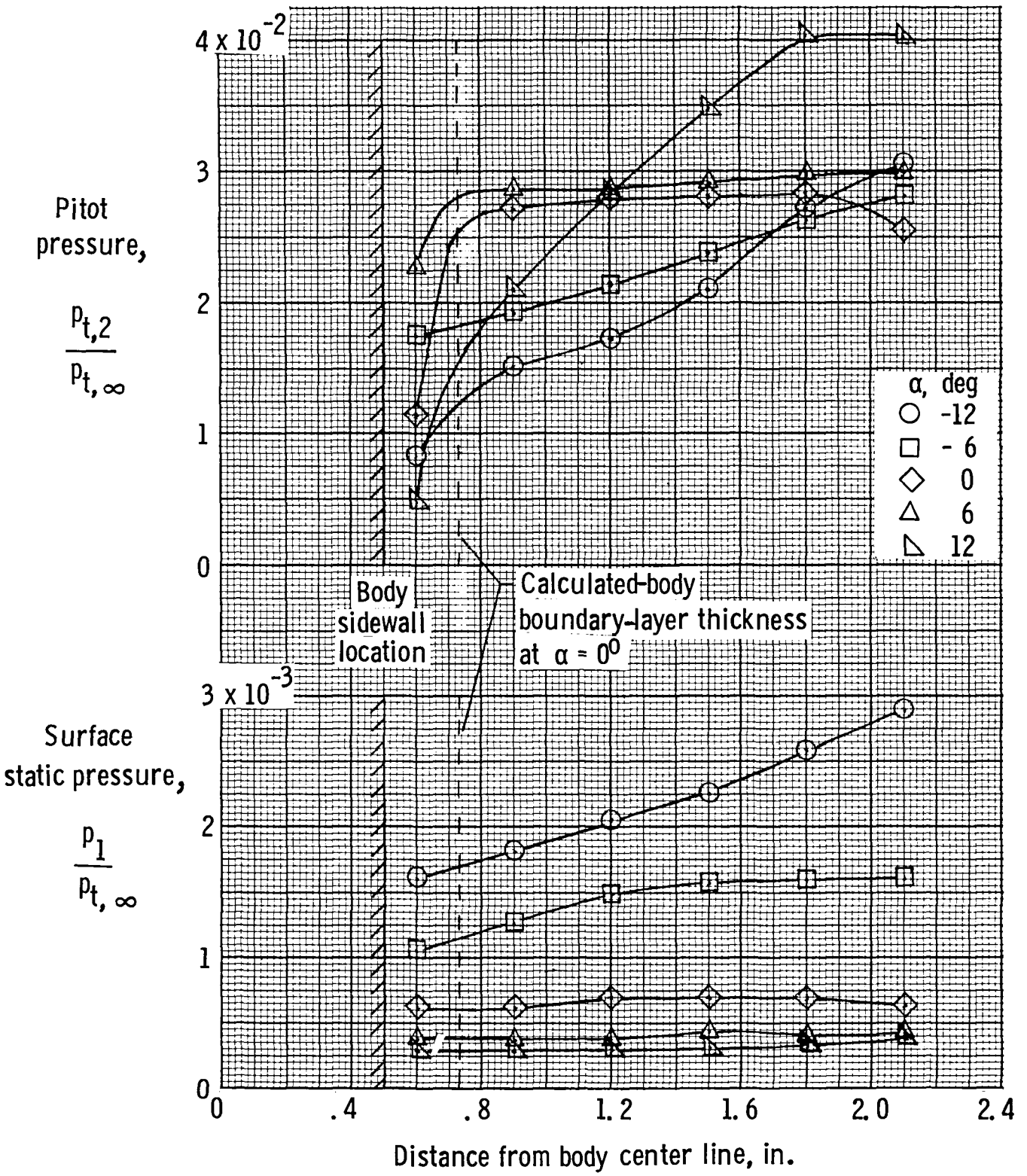

(c) Rectangular body and swept wing.

Figure 7.- Continued.

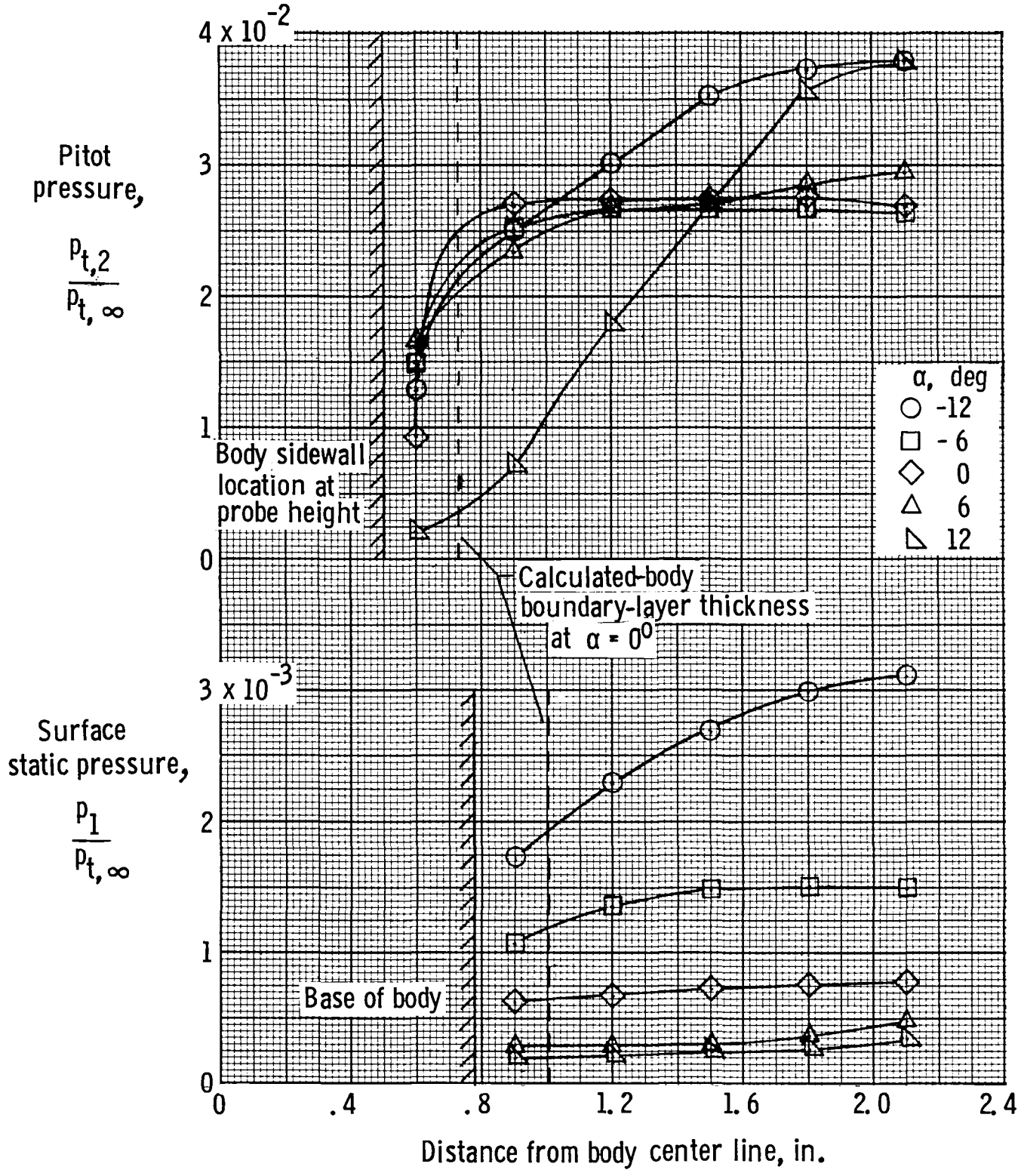

(d) Trapezoidal body and swept wing.

Figure 7.- Concluded.

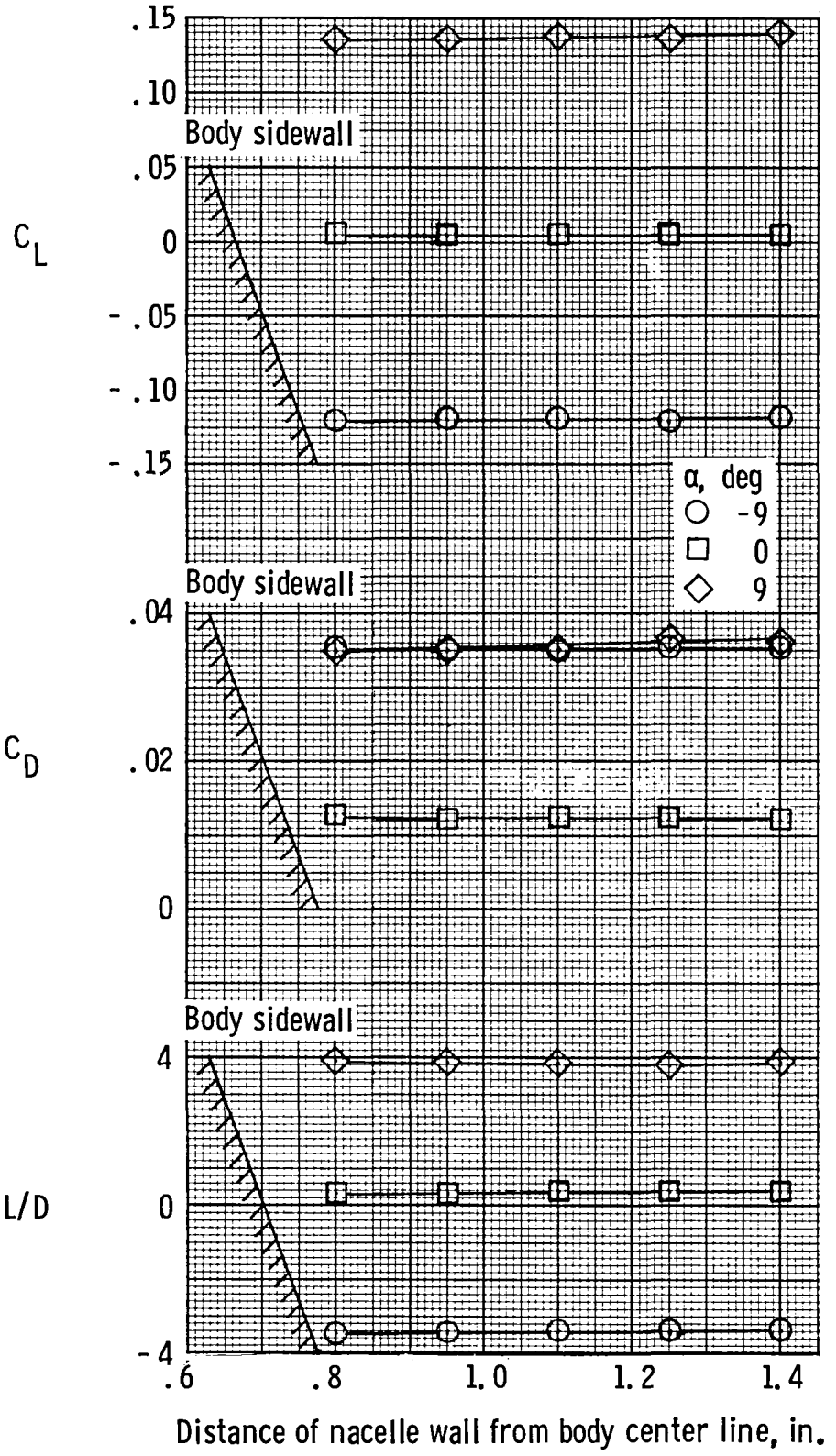

(a) Trapezoidal body and rectangular wing.

Figure 8.- Typical force data for lateral positions of nacelles.

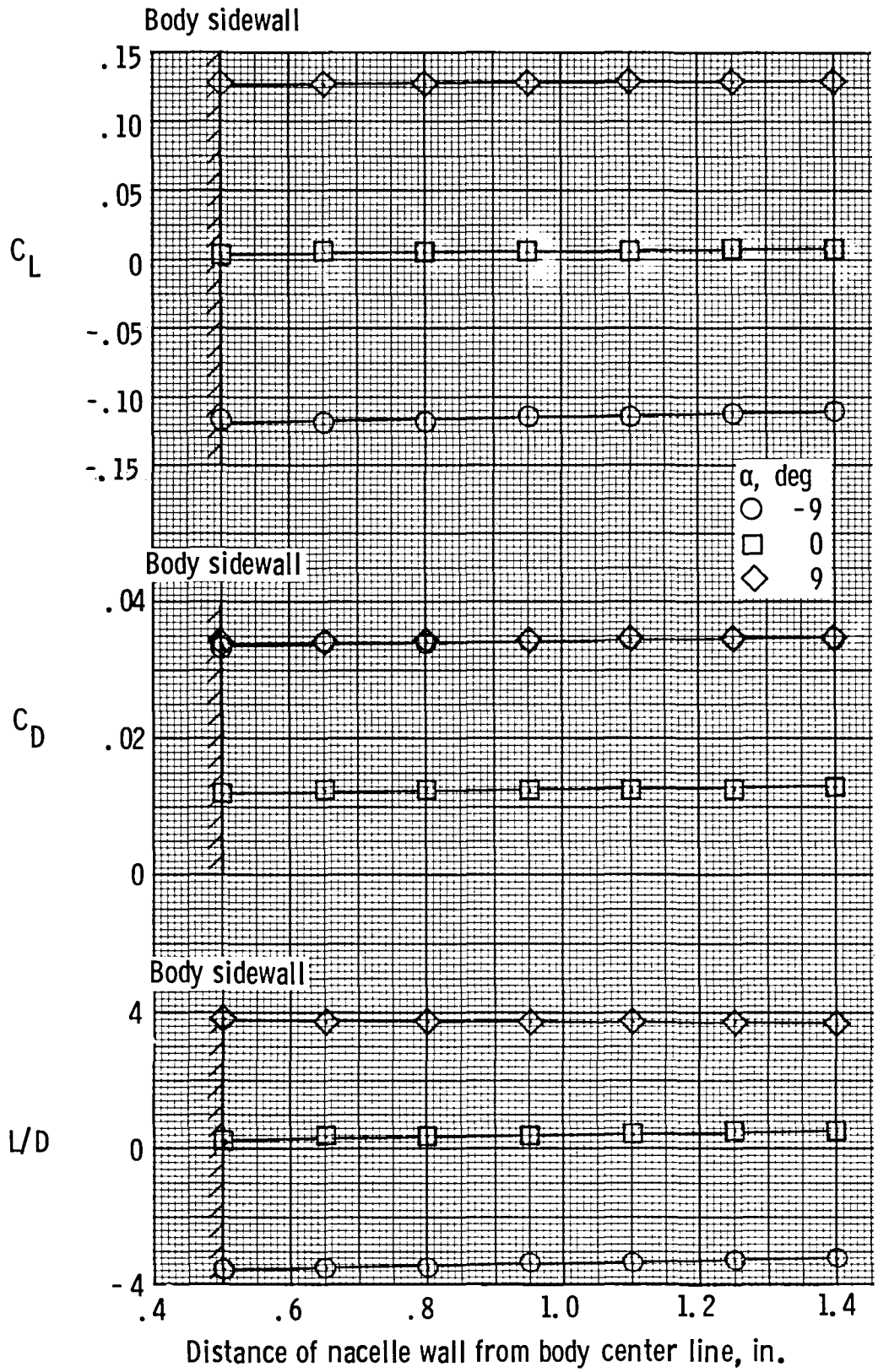

(b) Rectangular body and swept wing; nacelle inlets aft of wing leading edge.

Figure 8.- Concluded.

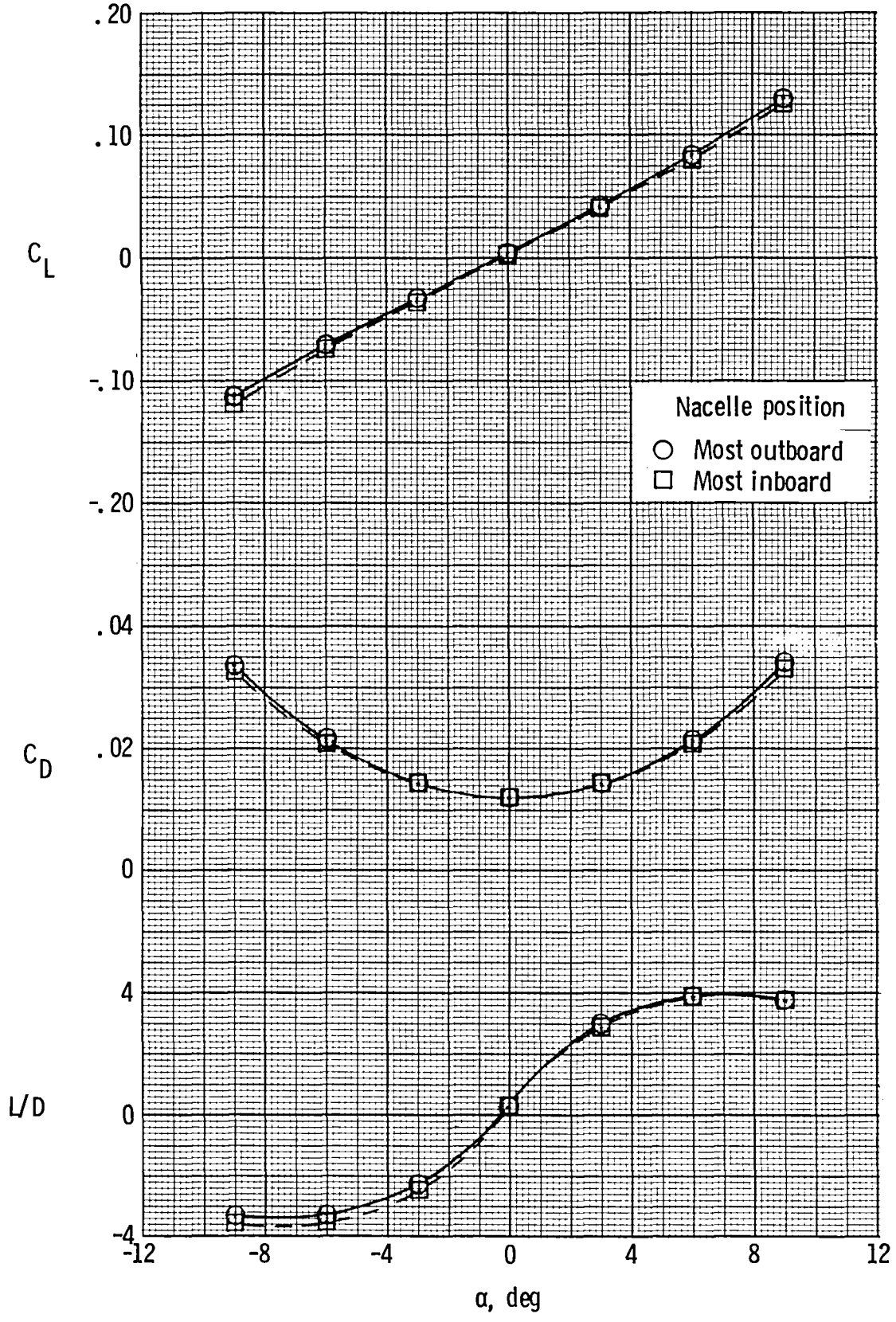

(a) Rectangular body and rectangular wing.

Figure 9.- Force data at most inboard and most outboard nacelle positions.

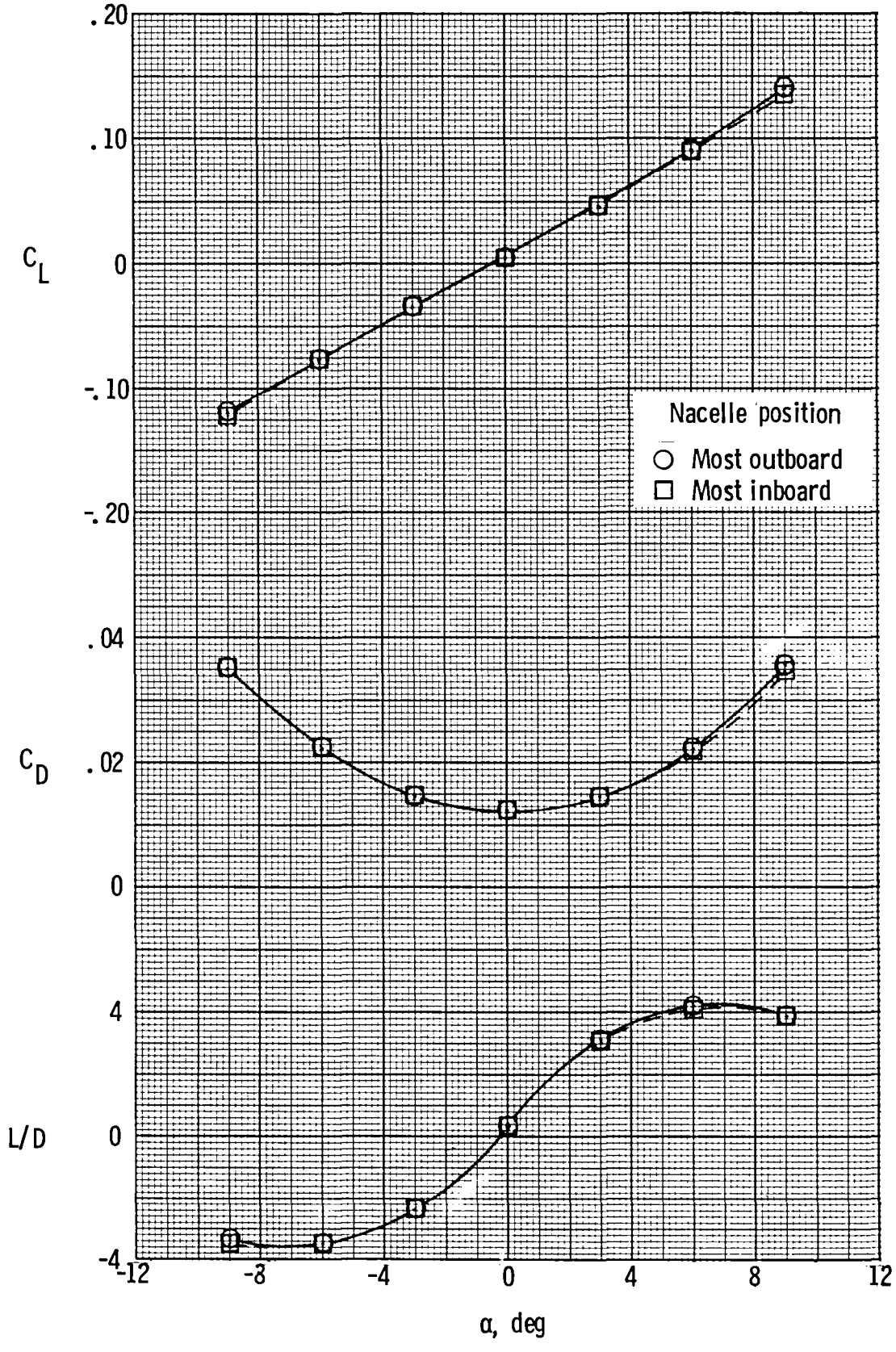

(b) Trapezoidal body and rectangular wing.

Figure 9.- Continued.

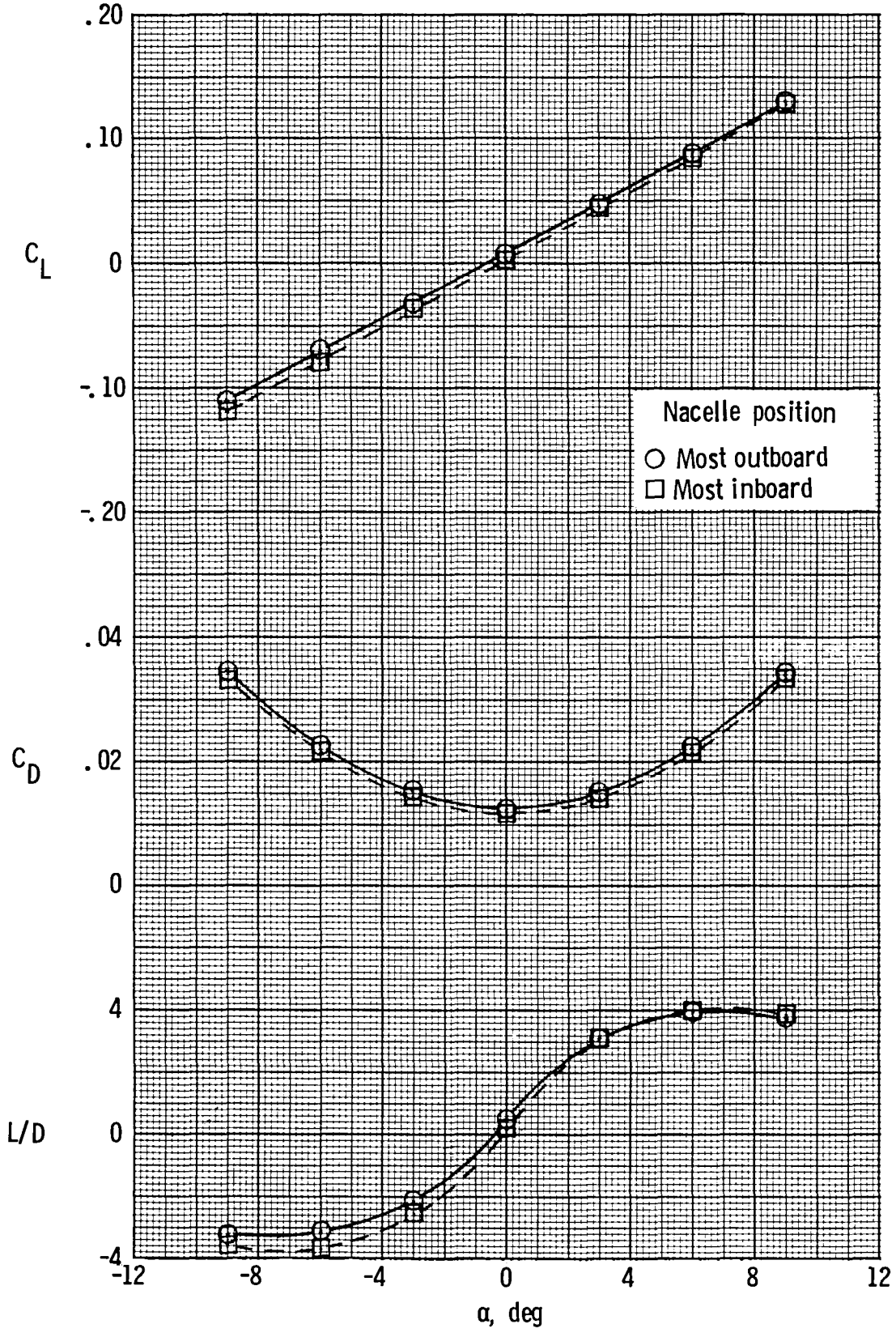

(c) Rectangular body, swept wing, and nacelle inlets aft of wing leading edge.

Figure 9.- Continued.

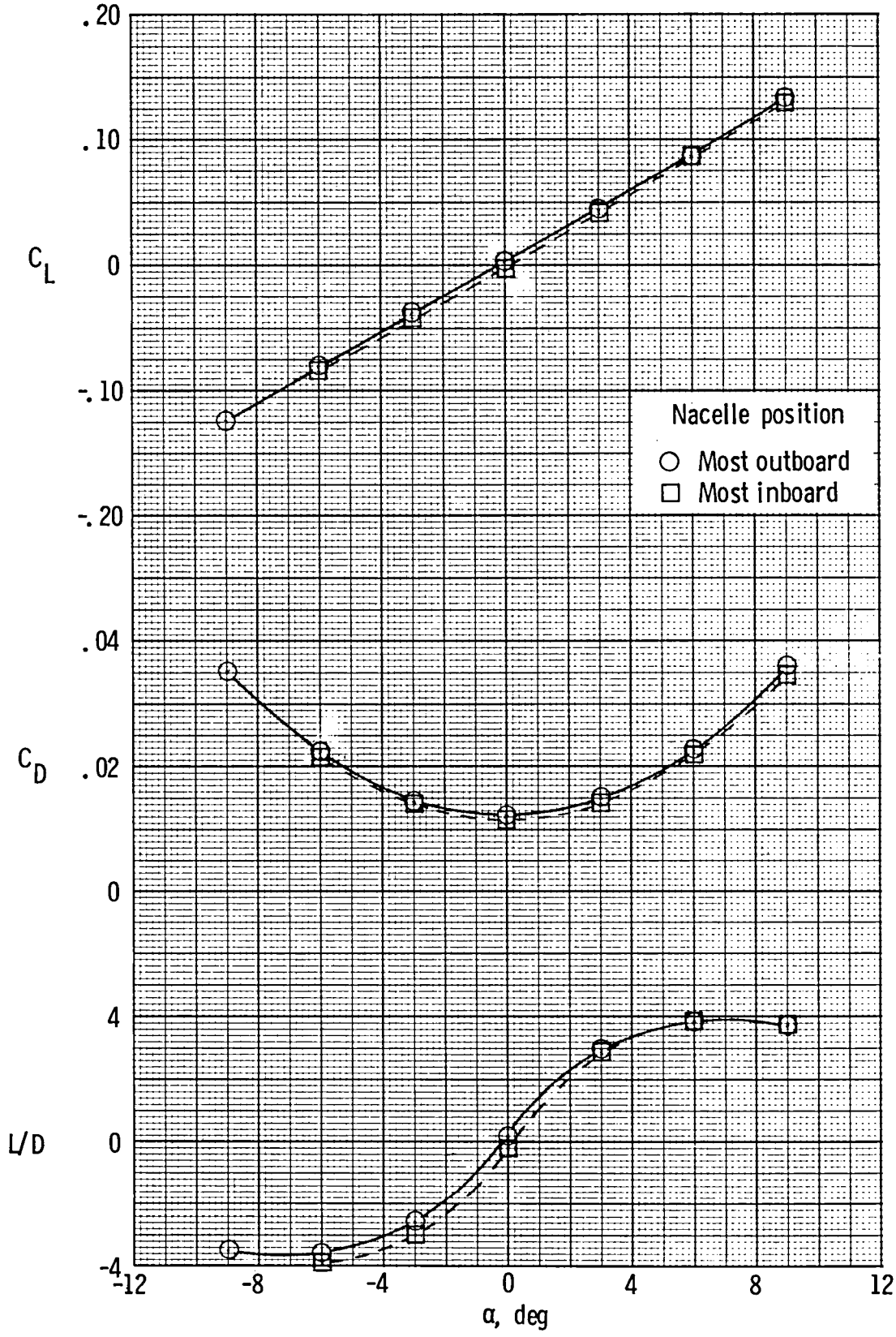

(d) Rectangular body, swept wing, and nacelle inlets forward of wing leading edge.

Figure 9.- Continued.

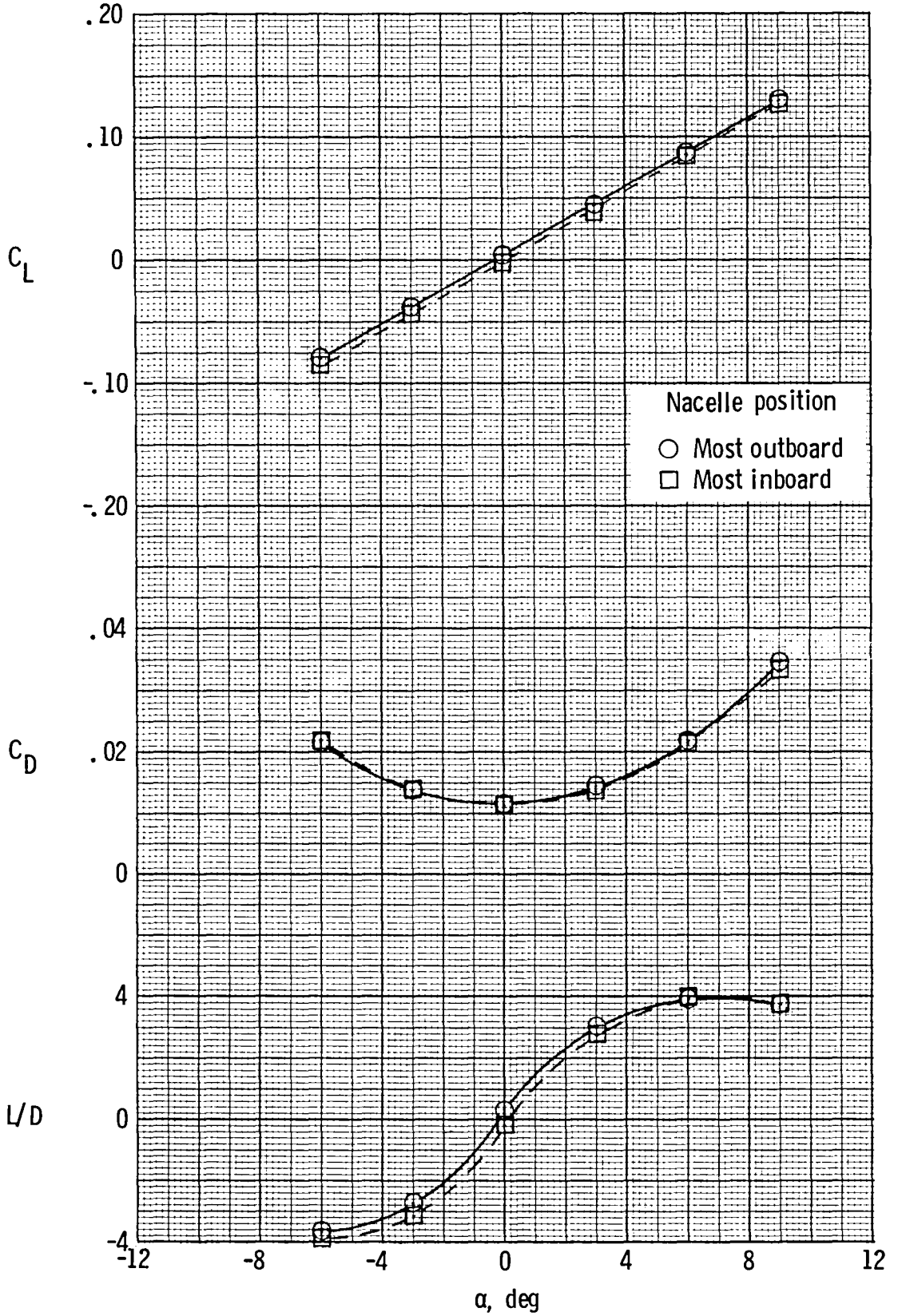

(e) Trapezoidal body, swept wing, and nacelle inlets forward of wing leading edge.

Figure 9.- Continued.

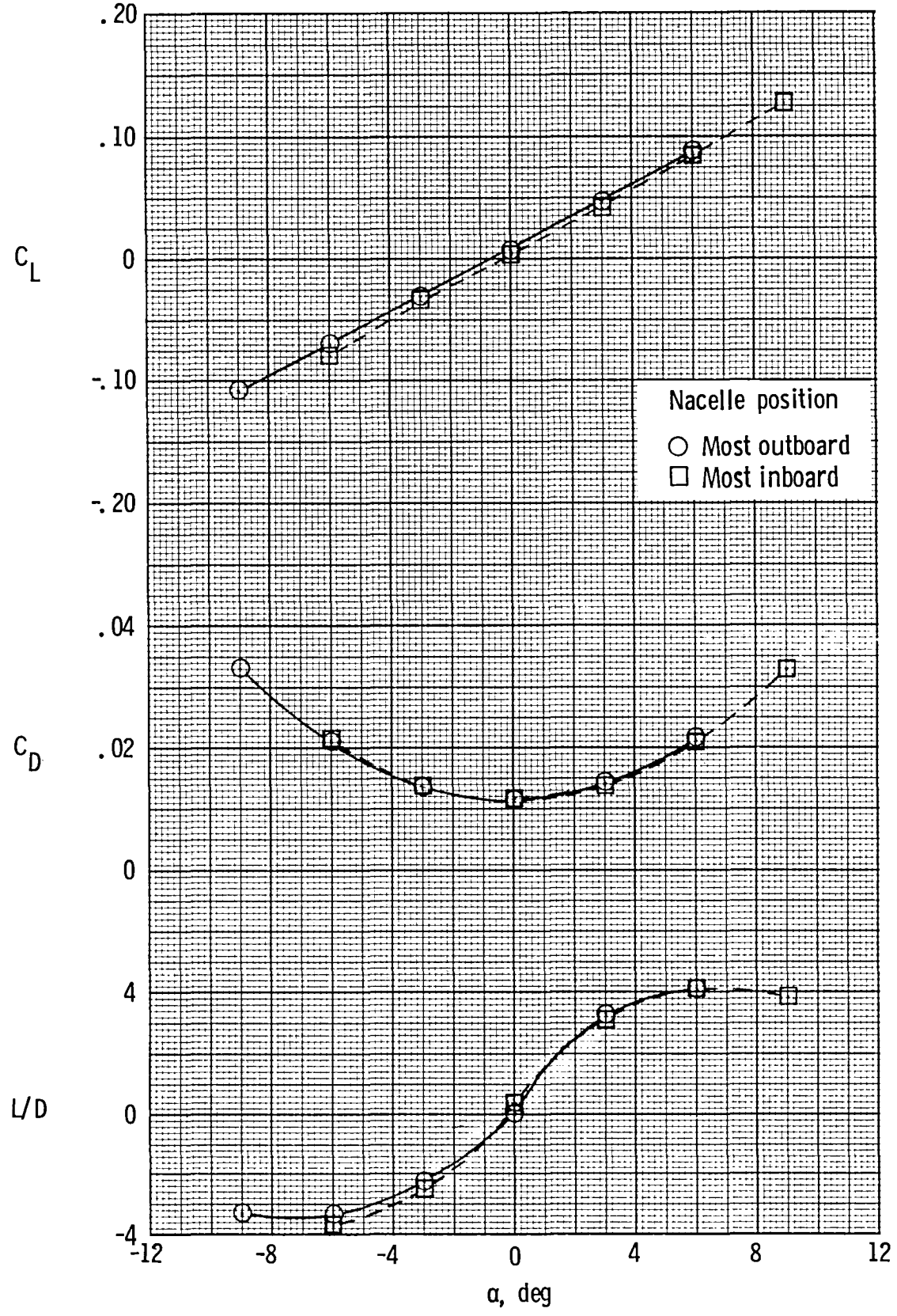

(f) Trapezoidal body, swept wing, and nacelle inlets aft of wing leading edge.

Figure 9.- Concluded.

1. Report No.	2. Government Accession No.	3. Recipient's Catalog No.
NASA TM-83287		

4. Title and Subtitle	5. Report Date
EXPERIMENTAL DETERMINATION OF FLOW-INTERFERENCE EFFECTS OF WING-MOUNTED, TWO-DIMENSIONAL, FULL-CAPTURE PROPULSION NACELLES IN CLOSE PROXIMITY TO A VEHICLE BODY AT A MACH NUMBER OF 6	May 1982
	6. Performing Organization Code: 505-43-83-01
7. Author(s): Walter A. Vahl	8. Performing Organization Report No.: L-15209
	10. Work Unit No.
9. Performing Organization Name and Address: NASA Langley Research Center, Hampton, VA 23665	11. Contract or Grant No.
	13. Type of Report and Period Covered: Technical Memorandum
12. Sponsoring Agency Name and Address: National Aeronautics and Space Administration, Washington, DC 20546	14. Sponsoring Agency Code

15. Supplementary Notes

16. Abstract

Experimental tests have been conducted to determine possible aerodynamic interference effects due to the lateral positioning of two-dimensional propulsion nacelles mounted on a wing surface in close proximity to a vehicle body. The tests were conducted at a Mach number of 6 and a Reynolds number of 7×10^6 per foot. The angle-of-attack range for force tests was -9° to 9°. The model configurations consisted of combinations of rectangular and trapezoidal cross-section bodies with a wing swept 65° and a rectangular planform wing. A pair of two-dimensional, flow-through propulsion nacelles simulated full-capture inlet operation.

17. Key Words (Suggested by Author(s))	18. Distribution Statement
Inlets Hypersonic propulsion Spillage Inlet interference Propulsion aerodynamics	Unclassified - Unlimited Subject Category 02

19. Security Classif. (of this report)	20. Security Classif. (of this page)	21. No. of Pages	22. Price
Unclassified	Unclassified	34	A03

For sale by the National Technical Information Service, Springfield, Virginia 22161

NASA-Langley, 1982

National Aeronautics and
Space Administration

Washington, D.C.
20546

Official Business
Penalty for Private Use, $300

THIRD-CLASS BULK RATE

Postage and Fees Paid
National Aeronautics and
Space Administration
NASA-451

NASA

POSTMASTER: If Undeliverable (Section 158
Postal Manual) Do Not Return